cambridge.org/jog

Post-Little Ice Age glacial lake evolution in Svalbard: inventory of lake changes and lake types

Iwo Wieczorek[1,2] ⓘ, Mateusz C. Strzelecki[2] ⓘ, Łukasz Stachnik[2,3], Jacob C. Yde[1] and Jakub Małecki[4]

[1]Department of Environmental Sciences, Western Norway University of Applied Sciences, Sogndal, Norway; [2]Alfred Jahn Cold Regions Research Centre, University of Wroclaw, Wroclaw, Poland; [3]German Research Centre for Geosciences, GFZ, Potsdam, Germany and [4]Cryosphere Research Group, Adam Mickiewicz University, Poznań, Poland

Abstract

The rapid formation of glacial lakes is one of the most conspicuous landscape changes caused by atmospheric warming in glacierised regions. However, relatively little is known about the history and current state of glacial lakes in the High Arctic. This study aims to address this issue by providing the first inventory of glacial lakes in Svalbard, focusing in particular on the post-Little Ice Age evolution of glacial lakes and their typology. To do so, we used aerial photographs and satellite imagery together with archival topographic data from 1936 to 2020. The inventory comprises the development of 566 glacial lakes (146 km^2) that were still in direct contact with glaciers during the period 2008–2012. The results show a consistent increase in the total area of glacial lakes from the 1930s to 2020 and suggest an apparent link between climatic and geological factors, and the formation of specific lake dam types: moraine, ice, or bedrock. We also detected 134 glacial lake drainage events that have occurred since the 1930s. This study shows that Svalbard has one of the highest rates of glacial lake development in the world, which is an indicator of the overall dynamics of landscape change in the archipelago in response to climate change.

1. Introduction

Glacial lakes are defined as 'bodies of water that are influenced by the presence of glaciers' (Fitzsimons and Howarth, 2018). It is important to note that we extend the definition of 'glacial lake' to include water bodies that are no longer fed by glacial water as a result of the complete disappearance of glaciers (Yao and others, 2018). Although this definition embraces supraglacial and subglacial lakes, some authors use the term 'glacial lakes' synonymously for lakes situated in proglacial environments. Glacial lakes are often divided into (1) ice-contact lakes and (2) ice-distal lakes (that is, not in direct contact with the glacier). Both types of glacial lakes are fed by glacial meltwater or the melting of inactive glacier ice and/or formed by glacial erosion or damming (Yao and others, 2018). In a warming climate with glacier retreat, ice-contact lakes are expected to develop into ice-distal lakes as glaciers retreat or disappear completely as a result of drainage (Fitzsimons and Howarth, 2018; Emmer and others, 2020, 2022; Shugar and others, 2020; Carrivick and others, 2020).

Glacial lakes are a component of many glacial landscapes (Carrivick and Tweed, 2013). In recent years, the number, size and volume of glacial lakes have changed rapidly worldwide as a result of climate-forced glacier recession (Veh and others, 2019; Shugar and others, 2020). There is also increasing awareness of the potential hazards of glacial lake outburst floods (GLOFs). This interest has led to the compilation of glacial lake inventories in many glacierised regions of the world, such as parts of the Himalaya (Ukita and others, 2011; Jain and others, 2012; Govindha Raj and others, 2013; Worni and others, 2013; Zhang and others, 2015; Govindha Raj and Kumar, 2016; Aggarwal and others, 2017; Chen and others, 2017; Prakash and Nagarajan, 2017; Govindha Khadka and others, 2018; Wang and others, 2020; Nie and others, 2017), the Karakoram Range (Senese and others, 2018; Mal and others, 2020), the Tibetan Plateau (Luo and others, 2020), the European Alps (Buckel and others, 2018), Greenland (How and others, 2021; Mallalieu and others, 2021), Alaska (Post and Mayo, 1970; Rick and others, 2022), the Andes (Loriaux and Casassa, 2013; Wilson and others, 2018) and Scandinavia (Andreassen and others, 2022). However, changes to glacial lakes in the High Arctic, where Arctic amplification enhances glacier recession (Rantanen and others, 2022), have received scant attention in contemporary studies owing to the absence of comprehensive lake inventories and the limited impact of GLOFs on settlements and infrastructure. The present inventory fills a gap in the existing global glacial lake database (Shugar and others, 2020), which generally lacks glacial lake analyses from the High Arctic regions because of the high level of cloud cover and the inferior quality of satellite images. Given the extremely rapid warming of the Barents Sea region (Isaksen and others, 2022), where Svalbard is situated, we can consider the archipelago as a unique laboratory for climate change impact on glacial

environments. An additional aspect emphasising the importance of research in Svalbard is that research conducted in this area has a long history and includes some of the longest observations of environmental change in the entire Arctic.

This study aims to classify and evaluate long-term changes to ice-contact glacial lakes, in the High Arctic of Svalbard since the termination of the Little Ice Age (LIA). We provide a comprehensive inventory of glacial lakes on Svalbard, including an overview of their spatial distribution and temporal changes (1936–2020).

2. Regional setting

The Svalbard archipelago lies between 74° N and 81° N and is surrounded by the Greenland Sea to the west and the Barents Sea to the east (Fig. 1). The archipelago consists of the larger islands Spitsbergen, Nordaustlandet, Edgeøya, Barentsøya, Kvitøya, Prins Karls Forland, Kong Karls Land, Hopen and Bjørnøya, along with several smaller islands. Svalbard is one of the regions in the Arctic where global warming is proceeding apace. The mean annual air temperature has increased by 4°C over the last 40 years (1979–2018) (Nordli and others, 2014; Isaksen and others, 2016; Wawrzyniak and Osuch, 2020). The current mean annual air temperature ranges from −5.2°C (Ny-Ålesund, north Spitsbergen) to −4.6°C (Longyearbyen, central Spitsbergen) and −4.3°C (Hopen Island, south-east Svalbard) (Førland and others, 2011). The average annual precipitation measured at the airport in Longyearbyen – the longest continuously operating weather station in Svalbard – is ∼ 190 mm, and with ongoing climate change, liquid or mixed (liquid-solid) precipitation is becoming more frequent at the expense of solid precipitation (Førland and Hanssen-Bauer, 2000; Førland and others, 2011). Climate projections indicate that the annual air temperature will rise by about 4–7°C, while the annual precipitation is expected to increase by about 45–65% (Moreno-Ibáñez and others, 2020).

Glaciers cover about 57% of the total area of Svalbard – about 34 000 km^2 (Nuth and others, 2013). The area of glaciers has been diminishing almost continuously since the maximum extent of the LIA, which occurred in the late 19th and early 20th centuries (Humlum and others, 2003; Farnsworth and others, 2016; Małecki, 2016; Noël and others, 2020; Schuler and others, 2020; Evans, 2011; Sobota and others, 2016; Sobota, 2014). Svalbard is dominated by polythermal glaciers containing cold and temperate ice (Hagen and others, 1993; Sevestre and others, 2015). Recent studies indicate that between 1936 and 2010, the total area of glaciers on Svalbard decreased by about 30% and that the mean thinning rates of glaciers varied between 0.3 and 0.5 m year^{-1}, depending on the region (Geyman and others, 2022). According to the Randolph Glacier Inventory (Pfeffer and others, 2014) about 15% of the area is drained by land-terminating glaciers. This subpopulation, representing about 85% of the total number of glaciers in Svalbard, is potentially capable of producing proglacial lakes as a result of marginal glacier retreat, typically at rates between 5 and 30 m year^{-1} (e.g. Rachlewicz and others, 2007; Małecki, 2016). In recent years, these glaciers have been displaying rapid thinning rates along west Spitsbergen and at Edgeøya (marginal thinning of 3–4 m/year) to more balanced conditions in the north and north-east (marginal thinning of 0.5–1 m year^{-1}) (Małecki, 2022).

The landscape of Svalbard is dominated mountain ranges, separated by deep *U*-shaped valleys and fjords (Dallmann, 2015). As a result of post glacial isostatic uplift, wide and relatively flat, raised marine terraces occupy the lower parts of the coastal landscape (Sessford and others, 2015; Strzelecki and others, 2017).

Knowledge of glacial lakes and their changes in Svalbard is limited. Well-studied glacial lake Goësvatnet in northern Sørkapp Land ceased to exist in 2001 due to retreat of Gåsbreen

and a glacial lake outburst flood (Grzes and Banach, 1984; Schoner and Schoner, 1997; Ziaja and others, 2016; Dudek and others, 2022). Other studies of glacial lakes in Svalbard relate to lake sediment records (e.g. Røthe and others, 2018; van der Bilt and others, 2019), water biogeochemistry (Holm and others, 2012; Ruman and others, 2021) or the development of sedimentological profiles at the bottom of lakes (Rajaram and others, 2023). Glacial lakes also act as important reservoirs that accumulate sediments from glaciers or Arctic catchments (Kavan and others, 2022). At present, however, there are no data on the number and area of glacial lakes in Svalbard or their spatial distribution and temporal changes.

3. Material and methods

3.1 Data compilation

To produce this inventory of the glacial lakes in Svalbard, we used various sources of remote sensing data (Table 1). Cloud cover was important for the correct identification of glacial lakes. Another factor was the appropriate selection of different data sources, enabling the fullest possible coverage of the whole of Svalbard: for this, we used various databases and aerial photographs. Due to emerging data gaps in individual time periods (resulting, for example, from too much cloud cover), our inventory additionally divided into glacial lakes of which we are able to trace the history of their changes over all the years analysed. This was thus appropriately defined as 'full coverage record'.

3.1.1 1936–1938
The earliest data come from archival aerial photographs taken by the Norwegian Polar Institute (NPI). These are oblique aerial photographs that enable the analysis of the Svalbard landscape between 1936 and 1938 (Norwegian Polar Institute, 2020a, 2020b). The photographs do not cover the entire surface area of Svalbard, however. The most conspicuous data gaps are over the eastern part of the island of Nordaustlandet, which is covered by an ice cap.

The high-resolution images from different angles, obtained along the coasts of Svalbard during this aerial campaign, yielded only scant coverage of the central part of the archipelago. This means that the presence of glacial lakes in the early 20th century cannot be accurately analysed. Additional difficulties are shadows cast by mountains, meteorological conditions such as high cloud cover, and the aircraft's irregular (surface-dependent) flight paths from which the images were taken (Norwegian Polar Institute, 2020a, 2020b). The accuracy of the analysis was enhanced by an orthophotomap created on the basis of 5507 of the photographs from the 1936–1938 aerial campaign (Geyman and others, 2022). As the resolution of this map is about 20 m it is not possible to analyse very small glacial lakes (smaller than about 1000 m^2). The map also has some georegistration errors (±100 m), which does not allow the positions of individual topographic objects to be precisely interpreted.

By simultaneously analysing the aerial photographs and the orthophotomap, we vectorised the glacial lakes in ArcMap; then, were able to analyse in detail the distribution and basic geometry of some glacial lakes in Svalbard. The smallest of these had an area of 1176 m^2 (Table 1). It is possible that lakes smaller than about 1000 m^2 existed during this period, but the quality of the available material precluded the inclusion of such small lakes in the inventory.

3.1.2 1990
We gained access to vectorised data from the 1990s from the NPI archive. The data cover the whole of Svalbard, including the state
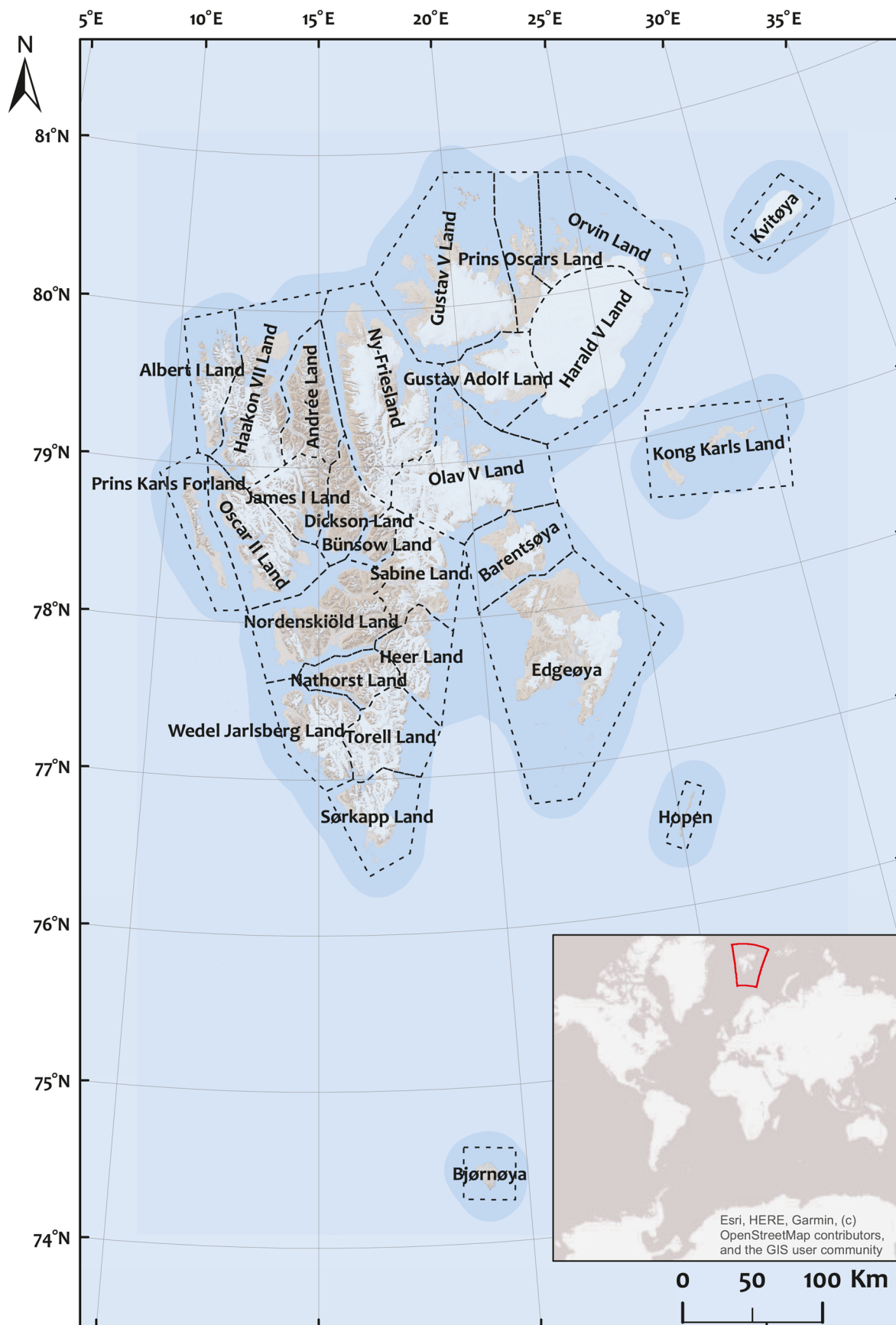
Figure 1. Map of Svalbard showing the regions used in this study.
Source: base map from Norwegian Polar Institute and ESRI.

of the glacial lakes in the late 20th century. Data were taken from the Svalbard topographic map 1: 100 000 (Norwegian Polar Institute, 2020a, 2020b). With the marked improvement in the quality of the material on which this analysis was based compared to the previous period, the smallest lake from the 1990s material was 317 m^2 in area.

Table 1. Summary of remote sensing data sources and types used to construct the inventory of glacial lakes

Year	Source	Type of remote sensing data	Minimum lake area [m^2]
1936–1938	NPI, Geyman and others (2022)	Orthophotomap checked with oblique aerial images	1177
1990s	NPI	Digitalised data and topographic map	317
2008–2012	NPI	Digitalised data checked with aerial images	320
2013–2019	Google Earth Pro (Landsat and Maxar)	Satellite images	145
2020	Sentinel satellite	Satellite images	1439

3.1.3 2008–2012

We examined the collection of aerial photos of Svalbard at 0.5 m resolution, taken by NPI during the 2008–2012 campaign, available via the online map service TopoSvalbard (Norwegian Polar Institute, 2020a, 2020b). We applied data from this period as a reference dataset for the inventory. The 2008–2012 campaign covered almost the entire archipelago apart from Torell Land, Wedel Jarlsberg Land, Nathorst Land, Heer Land, and the south-eastern part of Sabine Land, for which no glacial lake vector data from 2008 to 2012 were available. Where such vector data were missing, we analysed the available aerial photographs to obtain information regarding the presence of lakes during this period. The vector data of the period were created using much the same methods as for the 1990s. The accuracy is also based on the available topographic map and aerial photographs, and the smallest lake had an area of 320 m^2.

3.1.4 2013–2019

Data from Google Earth Pro yielded information on the state of the Svalbard landscape from 2013 to 2019. The images, derived from Google Earth Pro, free of cloud cover, translated into a mosaic of images compiled from different dates. The surface area and perimeter of individual lakes were directly obtained in Google Earth Pro using available tools. All the results were recorded in a summary table for comparing the evolution of glacial lakes (Table 2). Google Earth Pro mainly uses images from the Maxar and Landsat missions but does not mention the exact technical details of each image (apart from the date the image was taken). Their resolution also varies and is based mainly on the availability of a particular satellite scene and the atmospheric conditions on a given date. Owing to the incomplete satellite image coverage of Svalbard, this period was excluded in the analysis of lake dynamics, but we did include it in the supplementary material and described it briefly in the Results section. Based on the satellite scenes obtained from 2013–2019, the smallest of the inventoried lakes had an area of 145 m^2.

3.1.5 2020

The latest data in this study are from satellite images available from the Copernicus Sentinel-2 mission (https://sentinel2explorer.esri.com/). Because of the minimal cloud cover, we chose satellite images taken in August 2020 to obtain information about the state of Svalbard glacial lakes during the warmest month, when the snow cover was also the least. Only satellite images with less than 30% cloud cover were selected. After being checked for georeferencing, the satellite images were stitched together as an orthomosaic. In this way, we were able to review individual sites with potential glacial lakes during the inventory process and, by vectorising the water features found, enter them into the database. The quality of the free data available from Sentinel-2 for such a large area as Svalbard was relatively poor, so we were able to study only some of the glacial lakes indicated in the previous periods. Therefore, the smallest lake with information on the development of the geometry and area of the water bodies analysed had an area of 1439 m^2.

In order to reduce the margin of error made when examining these data, we simultaneously analysed the downloaded raster images in ArcMap software (with different resolutions from 10 to 20 m, depending on the region) and the raster images available in the Sentinel web browser with a 10 m resolution. Based on the raster mosaic of satellite scenes for the whole of Svalbard, we vectorised the glacial lakes in ArcMap software, thereby completing the range of quantitative data in this inventory.

3.2 Data processing

We performed the glacier lake analysis in five steps as shown in Figure 2. As a precondition, we focused the analysis on lakes in direct contact with glaciers in 2008–2012. This data series was chosen mainly because of the availability of high-resolution remote sensing data that covered almost the entire archipelago.

The first step was to select glacial lakes from among all the water bodies appearing in the NPI topographic objects database from 2008–2012. The automatic selection (ArcMap selection by attributes) was followed by a manual selection, which involved verifying the automatic results with the aid of aerial photos. This enabled supraglacial lakes to be excluded from the database and limited the potential risk of including nonglacial lakes (e.g. coastal lakes and lagoons, tundra lakes, post-glacial valley lakes). This may be a potential source of error when analysing poor-quality remote sensing data. All the analyses were carried out in ArcMap 10.7.1 software.

Table 2. Glacial lake types in Svalbard (2008–2012) categorised according to the classification schemes by Emmer and others (2016) and Yao and others (2018)

| Emmer and others (2016)	Class	Bedrock-dammed lakes			Ice-dammed lakes		Moraine-dammed lakes			Unclassified
Yao and others (2018)	Class Subclass	Glacial Erosion lakes			Ice-dammed lakes		Moraine-dammed lakes			-
		Cirque lakes	Glacial valley lakes	Other glacial erosion lakes	Advancing glacier-blocked lakes	Other glacier-blocked lakes	End (Frontal) moraine-dammed lakes	Lateral moraine-dammed lakes	Moraine thaw lakes	
Number		10	3	100	38	119	99	39	152	6
Total number		566								
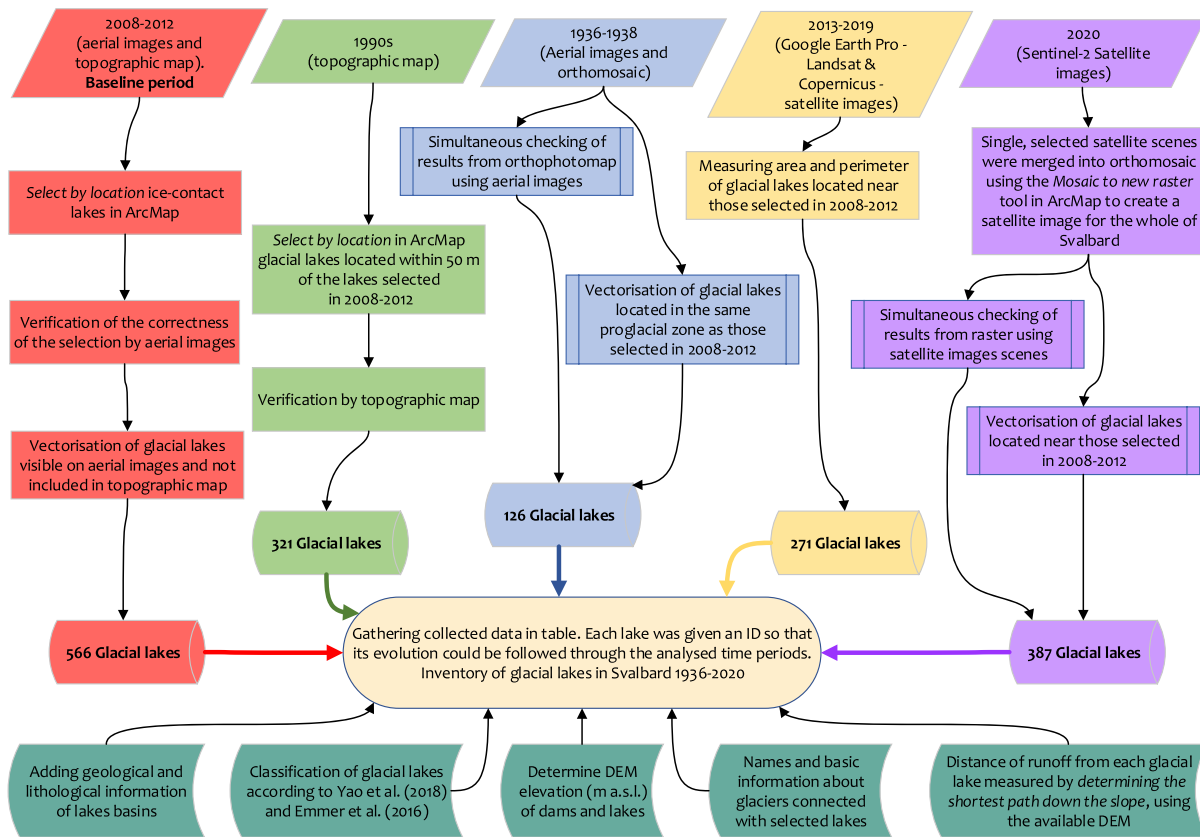
Figure 2. Flow chart showing the data compilation and processing.

In the second step, all the glacial lakes identified in 2008–2012 were checked for their presence in the 1930s. Qualitative data describing a lake's presence and its contact with glaciers, as well as quantitative data containing the area and perimeter of lakes, were accordingly recorded in an attribute table, which maintained a common identifier for each lake in all periods analysed. All glacial lakes were further verified by analysis of oblique aerial photographs from the 1936–1938 NPI flying campaign.

During the third step, the vectorised data from the 1990s (Table 1) were applied to selected glacial lakes situated in the same location as the lakes from the reference period (2008–2012). In addition to considering lakes that existed in the 1990s within the area occupied by glacial lakes in the 2008–2012 reference interval, we used a buffer that took into account water bodies located within 50 m of the reference period bodies in the selection process using ArcMap 10.7.1 software. Then the selected glacial lakes were quality-checked using the aerial photo data from 2008 to 2012.

The fourth step was to quality-check the glacial lakes selected from the reference period database using Google Earth Pro. If the quality of the images was such that analysis was possible, the areas of the glacial lakes were measured.

The final step of the data compilation involved vectorising the glacial lakes based on Sentinel images obtained in August 2020. The data collected (areas and perimeters) were added to the integrated attribute table, which enabled the inventory to be supplemented with data from 2020.

3.3 Measurement errors

To estimate the total measurement errors of the glacial lake area in Svalbard, the conventional error propagation technique was applied to the manually vectorised data from the 1930s, 1990s, 2008–2012 and 2020. The assumed uncertainty of horizontal lake outline vectorisation was different for individual periods, depending on the image precision and the data source. For data from the 1930s, we assumed a vectorisation uncertainty of ±20 m. The data from the 1990s was based on topographic map 1: 100 000 and 2008–2012 was based on high-resolution aerial imagery, so for these periods we assumed a vectorisation uncertainty of ±1 m. As the manual vectorisation was sometimes based on lower-resolution images (a margin of error of >10 m), the Sentinel data from 2020 was assessed as having a vectorisation uncertainty of ±20 m.

On completion of the vectorisation procedure, two area buffers with the assumed positive and negative vectorisation uncertainties were created around the lake outlines to estimate their higher and lower bounds of area measurement error. The average of the absolute differences between measured and buffered lake areas were set as the area measurement error of individual lakes. These were further used to calculate the total lake area measurement error for Svalbard and for all the time intervals in this study by means of the standard formula:

$$s = \sqrt{(a^2) + (b^2) + (c^2) + \ldots + (z^2)} \qquad (1)$$

where:

s – subregional/regional total lake area measurement error;
a, b, c, and z – measurement uncertainties for individual lakes within the region of interest.

We used Eqn 1 to obtain total lake area measurement errors for the entire area of Svalbard of the order of <1% for the periods 1990 and 2008/2012 and up to a few per cent for the remaining periods (Table 3). In addition, the average measurement uncertainty was differentiated with respect to the individual regions of Svalbard (Fig. 3).

Table 3. Long-term changes of glacial lakes in Svalbard with a full coverage record (1930s–2020) for analysed time periods

Region	Total area in 1936–1938 [km²]	Difference between 1936–1938 and 1990s [km²/%]	Total area in 1990s [km²]	Difference between 1990s and 2008–2012 [km²/%]	Total area in 2008–2012 [km²]	Difference between 2008–2012 and 2013–2019 [km²/%]	Total area in 2013–2020 [km²]	Difference between 2013–2019 and 2020 [km²/%]	Total area in 2020 [km²]	Difference between 1930s and 2020 [km²/%]	Normalised difference between 1930s and 2020 per 100 km² of land [km²]
Albert I Land	1.15	+0.37/+32%	1.52	+1.44/+94%	2.96	−0.26/−9%	2.70	+0.22/+8%	2.93	+1.78/+154%	+0.14
Andrée Land	0.00	+1.15/–	1.15	+5.82/+508%	6.97	+0.26/+4%	7.23	+0.36/+5%	7.59	+7.59/–	+0.33
Barentsøya	0.02	−0.02/−100%	0.00	+0.16/–	0.16	−0.05/−30%	0.11	+0.47/+426%	0.58	+0.56/+3461%	+0.04
Dickson Land	0.00	–	0.00	+0.02/–	0.02	+0.01/+62%	0.03	−0.03/−100%	0.00	0/–	0
Edgeøya	2.54	+3.38/133%	5.92	+13.91/+235%	19.83	+6.49/+33%	26.32	2.57/10%	28.89	+26.35/+1038%	+0.53
Gustav Adolf Land	0.09	+0.01/+13%	0.10	−0.01/−4%	0.09	+0.01/+5%	0.10	+0.01/+9%	0.11	+0.02/+24%	0
Gustav V Land	0.78	+1.78/+229%	2.56	+0.02/+1%	2.57	−0.90/−35%	1.68	+0.99/+59%	2.67	+1.89/+243%	+0.05
Haakon VII Land	0.00	+1.75/–	1.75	+0.86/+49%	2.62	0/0%	2.62	+0.36/+14%	2.98	+2.98/+−	+0.09
Heer Land	0.28	+2.98/+1060%	3.26	−3.26/−100%	0.00	+7.99/–	7.99	−3.42/−43%	4.57	+4.29/+1527%	+0.29
James I Land	0.02	+1.05/+5938%	1.07	+16.79/+1572%	17.86	+3.55/+20%	21.41	−6.00/−28%	15.41	+15.39/+86 984%	+0.76
Kong Karls Land	0.00	+0.43/+−	0.43	0/0%	0.43	−0.43/−100%	0.00	+0.16/–	0.16	+0.16/–	+0.05
Narthorst Land	0.19	+0.78/+405%	0.97	−0.97/−100%	0.00	+0.75/+−	0.75	−0.21/−29%	0.54	+0.034/+178%	+0.02
Nordenskiöld Land	0.19	+1.81/+975%	2.00	+0.28/+14%	2.28	+0.15/+7%	2.43	−0.31/−13%	2.12	+1.94/+1043%	+0.06
Ny-Friesland	15.34	+2.98/+19%	18.33	−2.66/−14%	15.67	+0.20/+1%	15.87	+2.27/+14%	18.14	+2.79/+18%	+0.06
Olav V Land	2.93	+0.43/+15%	3.36	+0.57/+17%	3.93	−0.18/−5%	3.75	+0.38/+10%	4.13	+1.20/+41%	+0.03
Orvin Land	7.37	−0.13/−2%	7.23	+0.77/+11%	8.00	−2.56/−32%	5.43	+0.33/+6%	5.77	−1.60/−22%	−0.09
Oscar II Land	0.00	+1.41/–	1.41	+3.20/+227%	4.60	+0.58/+13%	5.19	+0.52/+10%	5.70	+5.70/–	+0.22
Prins Oscars Land	5.14	−2.04/−40%	3.10	−0.14/−5%	2.96	−0.32/−11%	2.63	+0.61/+23%	3.24	−1.90/−37%	−0.18
Sabine Land	0.00	+0.64/+−	0.64	−0.22/−35%	0.42	+0.77/+185%	1.18	−0.53/−45%	0.65	+0.65/–	+0.02
Sørkapp Land	0.00	+0.17/–	0.17	+0.42/+242%	0.60	−0.36/−60%	0.24	−0.16/−68%	0.08	+0.08/–	+0.01
Torell Land	0.14	+0.14/+101%	0.28	−0.28/−100%	0.00	+0.37/–	0.37	+0.18/+48%	0.56	+0.42/+294%	+0.02
Wedel Jarlsberg Land	4.34	+1.58/+36%	5.91	−5.91/−100%	0.00	+6.76/–	6.76	−1.42/−21%	5.34	+1.00/+23%	+0.05
Total	**40.50**	**+20.65/+51%**	**61.16**	**+30.80/+50%**	**91.96**	**+18.96/+21%**	**110.92**	**+1.22/+1%**	**112.14**	**+71.64/+177%**	+0.09
Error propagation [km²]	±0.98		0.04		0.1		–		1.19		

3.4 Inventory features

The information extracted from the data sources was compiled and grouped in the final inventory. We extended the metadata by including information about the regions in which the individual lakes are located (Dallmann, 2015) and about the lithology based on geokart.npolar.no – Geology. The Digital Elevation Model (DEM) has a resolution of 20 m and is made up of DEMs created for separate smaller areas of Svalbard on various dates in 2011. The model was finally published in 2014 (Norwegian Polar Institute, 2020a, 2020b). Based on the DEM provided by NPI, the heights above sea level of the individual lakes and their dams were recorded by creating the centroids of the objects in ArcMap 10.7.1. Based on the Glacier Atlas of Svalbard and Jan Mayen and TopoSvalbard, information on each of the glaciers that came into direct contact with the lakes was recorded (Hagen and others, 1993).

Using the spatial statistics tools available in ArcMap 10.7.1, we determined the directional distribution of individual glacial lake classes relative to the geology of Svalbard. According to definition of this tool it *creates standard deviational ellipses to summarise the spatial characteristics of geographic features: central tendency, dispersion, and directional trends.*

All the lakes were classified on the basis of their dam properties by applying the classifications of Emmer and others (2016) and Yao and others (2018). The classification of Emmer and others (2016) is less detailed than that of Yao and others (2018) as it only divides lakes into classes, while Yao and others (2018)'s the latter includes a subclass division (Table 2). Applying a unified classification scheme makes it possible to group glacial lakes into those that potentially exhibit increased seasonal changes and those that will drain only during GLOF events. The biggest challenge with regard to the Emmer and others (2016) and Yao and others (2018) classifications was to identify bedrock-dammed lakes using remote sensing tools. Emmer and others (2016) call these glacial lakes 'bedrock-dammed lakes', whereas the term 'glacial erosion lakes' is used by Yao and others (2018).

To obtain additional data, we compared the altitudes of the glacial lakes above sea level between the first and last years of the periods analysed (1936–2020). We aggregated lakes into increments of 50 m altitude intervals before performing an exponential fitting in MS Excel software.

4. Results

4.1 Glacial lake typology and change inventory

The Svalbard glacial lake inventory contains 566 lakes that were present during the reference period (2008–2012) (Fig. 5). 560 of
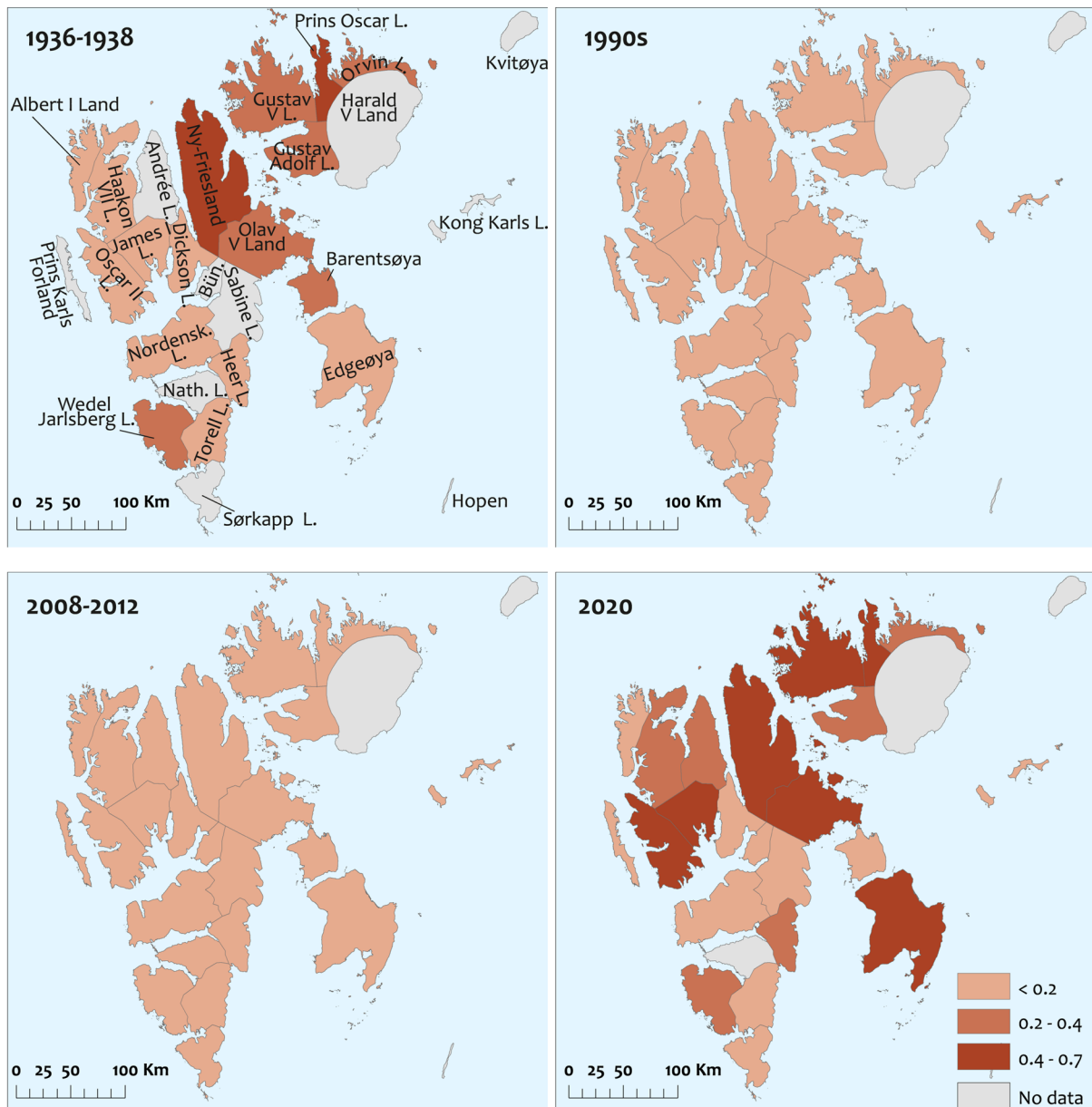
Figure 3. Uncertainty of lake area assessment for the period 1930s–2020.
Source: base map from Norwegian Polar Institute.

these lakes are included in Table 2; the other six are not categorised in light of the criteria selected for comparing lakes according to the classifications by Emmer and others (2016) and Yao and others (2018) (Fig. 4). The six unclassified glacial lakes make up a tiny minority and are therefore not considered in the following analysis.

On the basis of these lake classifications, moraine-dammed lakes represent more than half of all glacial lakes in Svalbard (290) (Figs 5 and 6a), followed by ice-dammed lakes (157) (Fig. 6b), whereas bedrock-dammed lakes constitute less than 20% of them (113) (Fig. 6c). The region with the greatest number of glacial lakes is Ny-Friesland (north-east Spitsbergen), while that with the fewest is Bünsow Land in central Spitsbergen (Fig. 4). Moraine-thaw lakes (sensu Yao and others, 2018), also known as moraine thermokarst lakes (Coulombe and others, 2022) (Fig. 6a) are the most common type of moraine-dammed lakes formed in the marginal zones of Svalbard glaciers (152). The 99 frontal moraine-dammed lakes (Fig. 6a) and the 39 lateral moraine-dammed lakes are the other subgroups of moraine-

dammed lakes (Fig. 6a; Table 2). The 157 ice-dammed lakes lie mainly in north-east Spitsbergen and between two ice caps on the island of Nordaustlandet (Fig. 6b). The ice-dammed lakes (157) can be categorised into 38 advancing-glacier ice-dammed lakes (Fig. 6b) and 119 other ice-dammed lakes. (Fig. 6b; Table 2). The 113 bedrock-dammed lakes are situated primarily on Nordaustlandet and in the northern part of Ny-Friesland (Fig. 6c). As it is often difficult to identify bedrock-dammed lakes from remote sensing data, the classification of some of these lakes should be validated by field observations. Using the classification of Yao and others (2018), we distinguished ten cirque lakes (Fig. 6c), three glacial valley lakes (Fig. 6c) and 100 other glacial erosion lakes (Fig. 6c; Table 2).

Our classification shows a specific spatial pattern in the distribution of different classes of glacial lakes across Svalbard. The largest number of bedrock-dammed lakes occurs in Nordaustlandet (58%), whereas 38% are in north Spitsbergen and 4% in south Spitsbergen. This contrast with the distribution of ice-dammed lakes, where 54% are in north Spitsbergen and 26 and 13% are
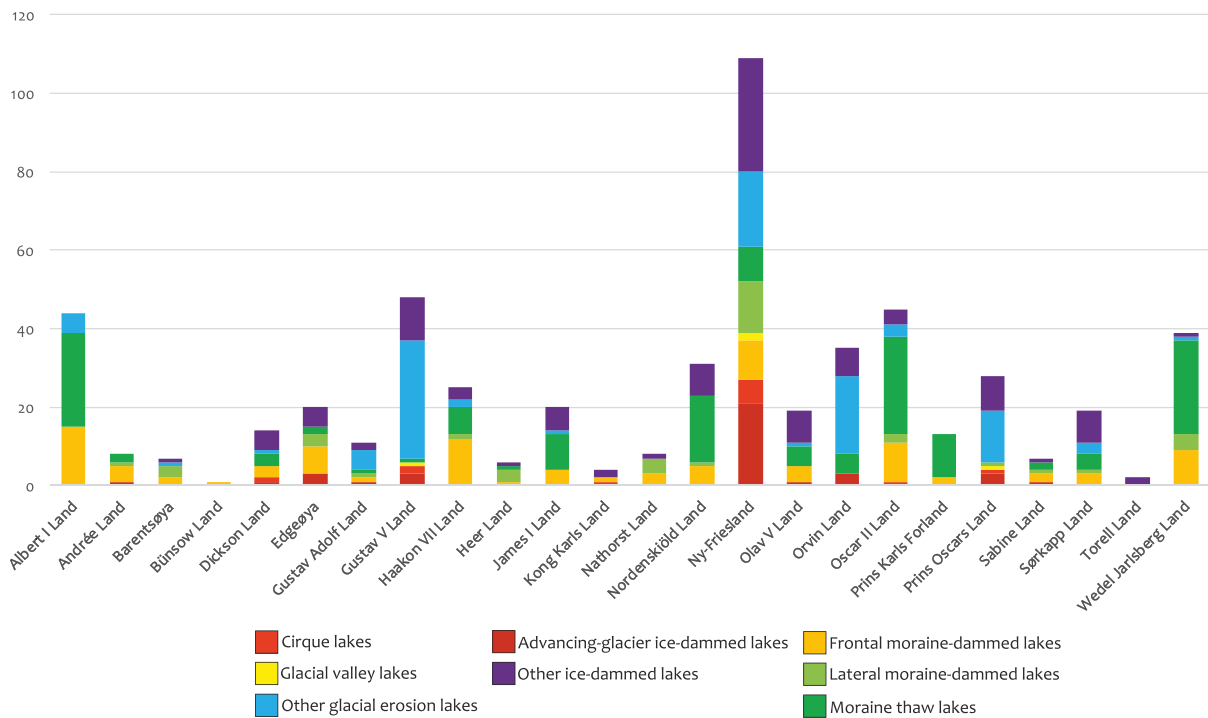
Figure 4. Classification of glacial lakes in different regions of Svalbard.

in Nordaustlandet and south Spitsbergen, respectively. Most moraine-dammed lakes are in north Spitsbergen (58%) and south Spitsbergen (28%), whereas Edgeøya and Prins Karls Forland each have 4% of the moraine-dammed lakes.

We have shown that between the 1930s and 2020 there is a 1.7-fold (or 72 km^2) increase in the total area of the lakes with full coverage record in Svalbard (Table 3). By full coverage record, we mean glacial lakes that were observable in all records examined. The largest changes in the number of glacial lakes took place in north Spitsbergen (Fig. 7), where 43 lakes existed in the 1930s, 120 in the 1990s, and 112 between 2008 and 2012. For lack of data of the appropriate quality for the entire island of Nordaustlandet, only 61 of the 294 glacial lakes there were identified from 2013 to 2019. However, the Sentinel data showed that there were 169 lakes on the island in 2020.

To better represent the changes of glacial lakes that have occurred in Svalbard, we have selected only those lakes for which we have full coverage records (1936–2020) for direct analysis. This data subset, listed in Table 3, indicates that a pronounced increase in glacial lake area occurred between the 1990s and 2008–2012. It is important to note that the analysis of the full years of data (1936–2020) differs from that of other years with incomplete data. Because our aim is to demonstrate the trends in Svalbard, we will focus on the analysis of the full coverage records.

Changes in the area of glacial lakes over the time intervals revealed an additional trend, showing that the extent of lake drainage was the largest between 2013–2019 and 2020 (about 12 km^2, 2.7% per dec) and the smallest between the 1930s and 1990s (about 5 km^2, 0.2% per dec). In contrast, the largest increase in the total area of glacial lakes occurred between the 1990s and 2008–2012 (about 46 km^2, 5% per dec) and the smallest between 2013–2019 and 2020 (about 16 km^2, 3.5% per dec). As regards the overall development of glacial lakes on Svalbard, there was a continuous increase in the area of these lakes between 1936 and 2020 (about +72 km^2, +177%). The analysis shows that the greatest changes in the area of glacial lakes (1936–2020) took

place on Edgeøya and in James I Land, where the glacial lake area increased by over 10 km^2 (Table 3). In contrast, the largest decreases in glacial lake area were recorded in Prins Oscars Land and Orvin Land, where the loss was more than 0.5 km^2. For better comparison of our results, we also normalised the changes that occurred between 1936 and 2020 in the surface area of glacial lakes per 100 km^2 of each region (Table 3). The largest changes in lake surface areas in the different Svalbard regions occurred in James I Land (+0.76 km^2) and the smallest in Sørkapp Land (0.01 km^2). The largest decrease in lake area was recorded in Prins Oscars Land (−0.18 km^2). Figure 8 shows examples of three moraine-dammed lakes located on Svalbard, where a significant increase in area has been observed in recent years.

Owing to the diverse bedrock geology of Svalbard, we prepared basic spatial statistics showing certain dependencies between the lithology and the type of glacial lake (Table 4, Fig. 9). Moraine-dammed lakes, which are found primarily on the west coast of Spitsbergen, lie mainly on unconsolidated and sedimentary rock substrates. Ice-dammed lakes predominate on the metamorphic rocks in north-eastern Spitsbergen and central Nordaustlandet. On igneous rocks, we have bedrock-dammed lakes in Nordaustlandet, but they are few of them in comparison with the other types of lakes. In addition, we took into account the distribution of the individual glacial lake types in relation to the entire archipelago and indicated their spatial distribution axis using the spatial statistics tool 'directional distribution', shown in Figure 9.

During all the time periods, 75% of the glacial lakes lay at elevations between 0 and 50 m a.s.l. (Fig. 10a–e). Only the 1930s stand out in this case, when the number of lakes in Svalbard was almost similar across the different altitude ranges from 0 to 250 m a.s.l. From the 1930s to 2020, the number of glacial lakes above 250 m a.s.l. decreased significantly, whereas from 251 to 400 m a.s.l. this number remained much the same. Above 401 m a.s.l., there was a small increase. Above 650 m a.s.l., the number of glacial lakes fell to a few occurring even at heights above 1042 m a.s.l.
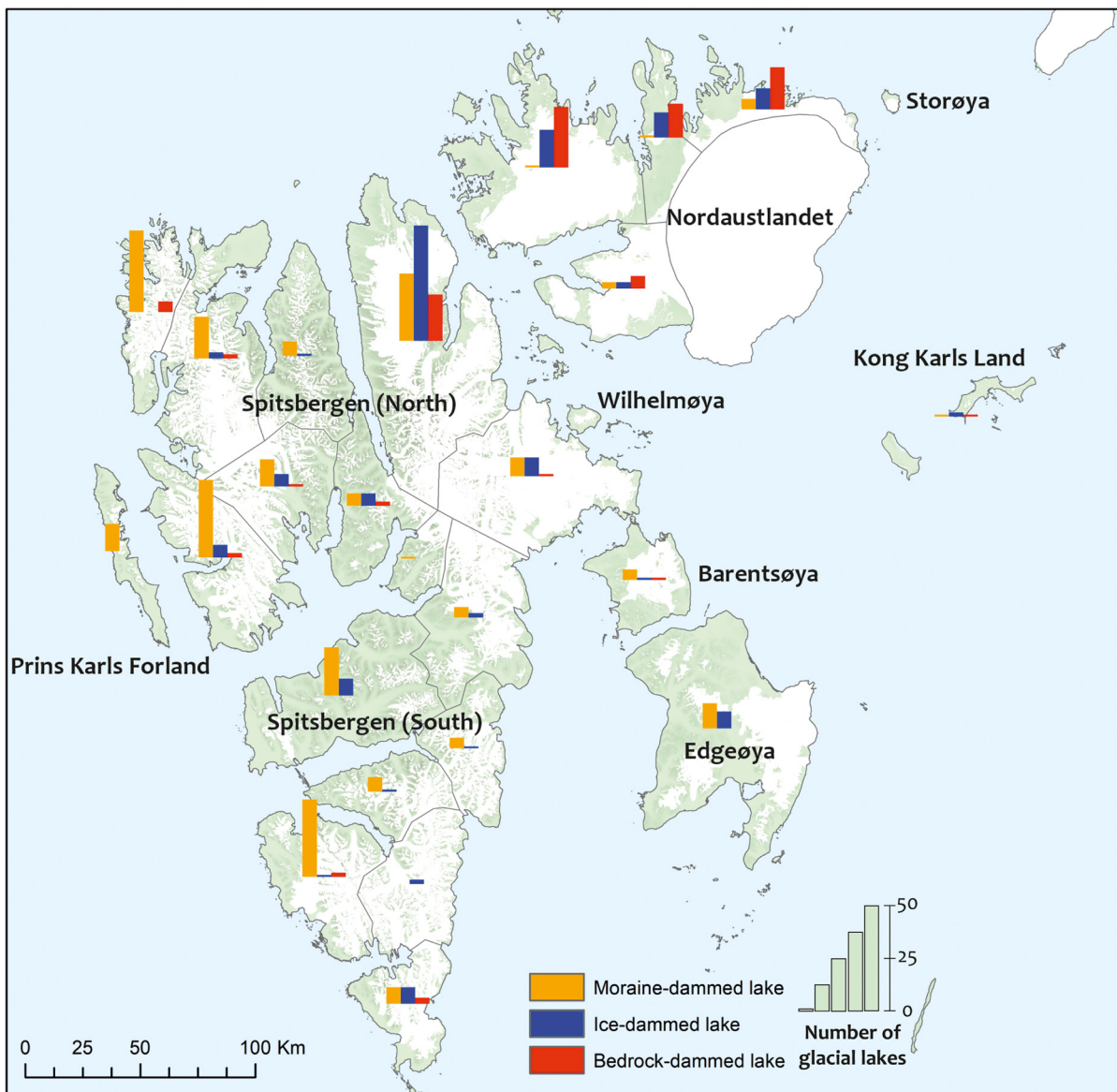
Figure 5. The distribution of glacial lake types in Svalbard based on the classification by Emmer and others (2016). Source: base map from Norwegian Polar Institute.

4.2 GLOF inventory

Comparison of the available data from the areas of glacial lake changes between 1936 and 2020 shows the historical occurrences of glacial lake drainage events based only on remote sensing data. In total, there were 25 such events identified between 1936 and the 1990s, 39 between the 1990s and 2008–2012, 30 between 2008–2012 and 2013–2019, and 40 between 2013–2019 and 2020 (Figs 10f and 11). For a more accurate interpretation of the results, we normalised the lake drainage events per decade, as follows: there were 4 between 1936 and the 1990s, 26 between the 1990s and 2008–2012, 50 between 2008–2012 and 2013–2019, and 100 between 2013–2019 and 2020.

We have to take into consideration the possibility that while we probably determined glacial lake drainage events that occurred between the 1990s and 2020, lake drainage between the 1930s and 1990s could also have occurred slowly and lasted for several years. However, for lack of an adequate range of data from the first half of the 20th century, this is the only possible method of estimating the minimum number of lake drainage events in the first half of the 20th century and thereafter until the 1990s. Over the entire period from the 1930s to 2020, there were at least 16 drainage events from bedrock-dammed lakes, 53 from ice-dammed lakes and 65 from moraine-dammed lakes.

We have also indicated at what altitude above sea level the lake drainage events included in our inventory originated. The highest number of recorded drainage events occurred from lakes at altitudes between 0 and 150 m a.s.l. Lakes situated up to 300 m a.s.l. were less active in this respect, and above this altitude only a few such events (less than 10) are known to have taken place. The highest-lying lake showing increased drainage activity was situated at 701–750 m a.s.l. (Fig. 10f).

5. Discussion

This first inventory of glacial lakes in Svalbard characterises the mechanisms controlling lake formation, growth and changes over time. Our dataset spans a period of more than 80 years, during which time Svalbard glaciers have retreated significantly from their maximum positions in the LIA, which came to an end at the turn of the 20th century. Until the mid-1980s, the glaciers on
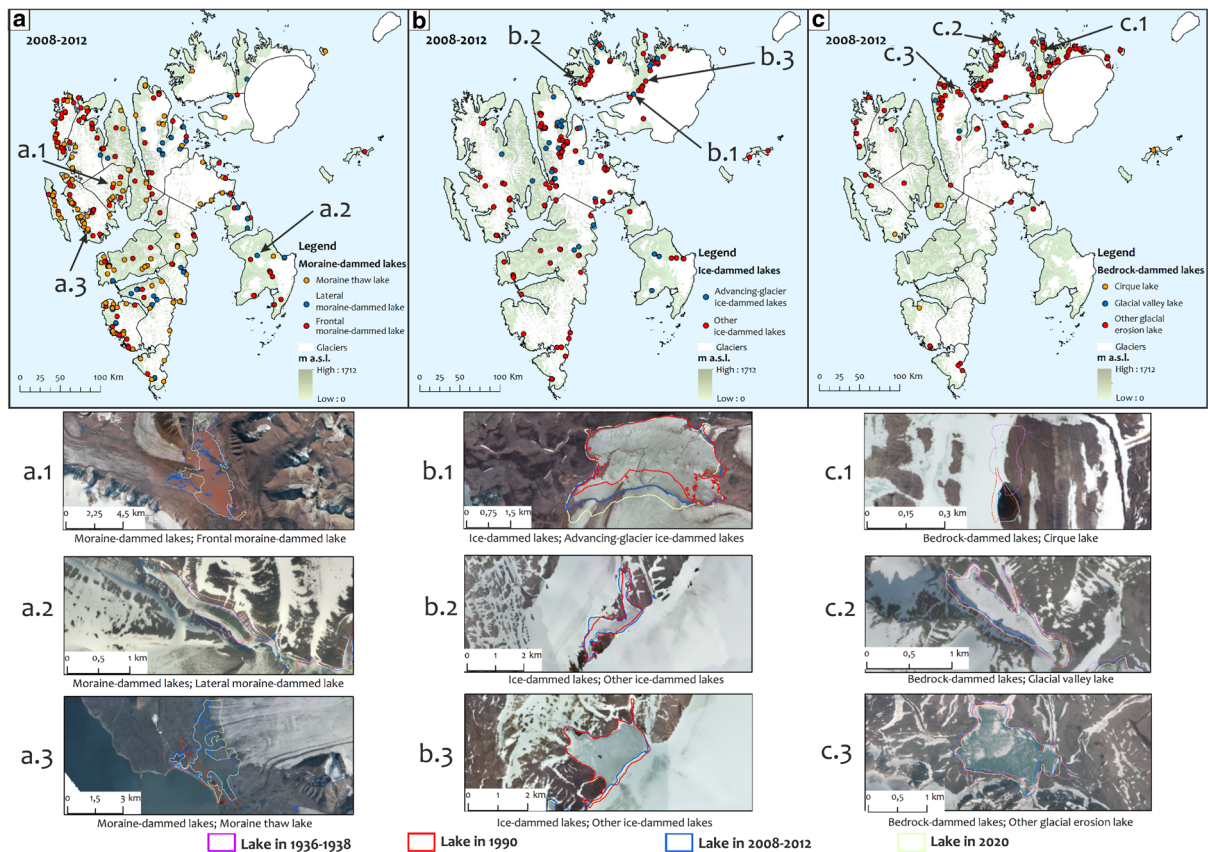
Figure 6. Spatial distribution of (a) moraine-dammed lakes in Svalbard: (a.1) frontal moraine-dammed lake at Holmströmbreen, Morabreen and Orsabreen, (a.2) lateral moraine-dammed lake at Storskavlen, (a.3) moraine-thaw lake at Eidembreen; (b) ice-dammed lakes in Svalbard: (b.1) advancing-glacier ice-dammed lake at Etonbreen, (b.2) other ice-dammed lake at Backabreen, (b.3) other ice-dammed lake at Flòtbreen; (c) bedrock-dammed lakes in Svalbard: (c.1) cirque lake, (c.2) glacial valley lake at Longstaffbreen, (c.3) another glacial erosion lake at Buldrebreen.
Source: base map from Norwegian Polar Institute and Sentinel satellite images.
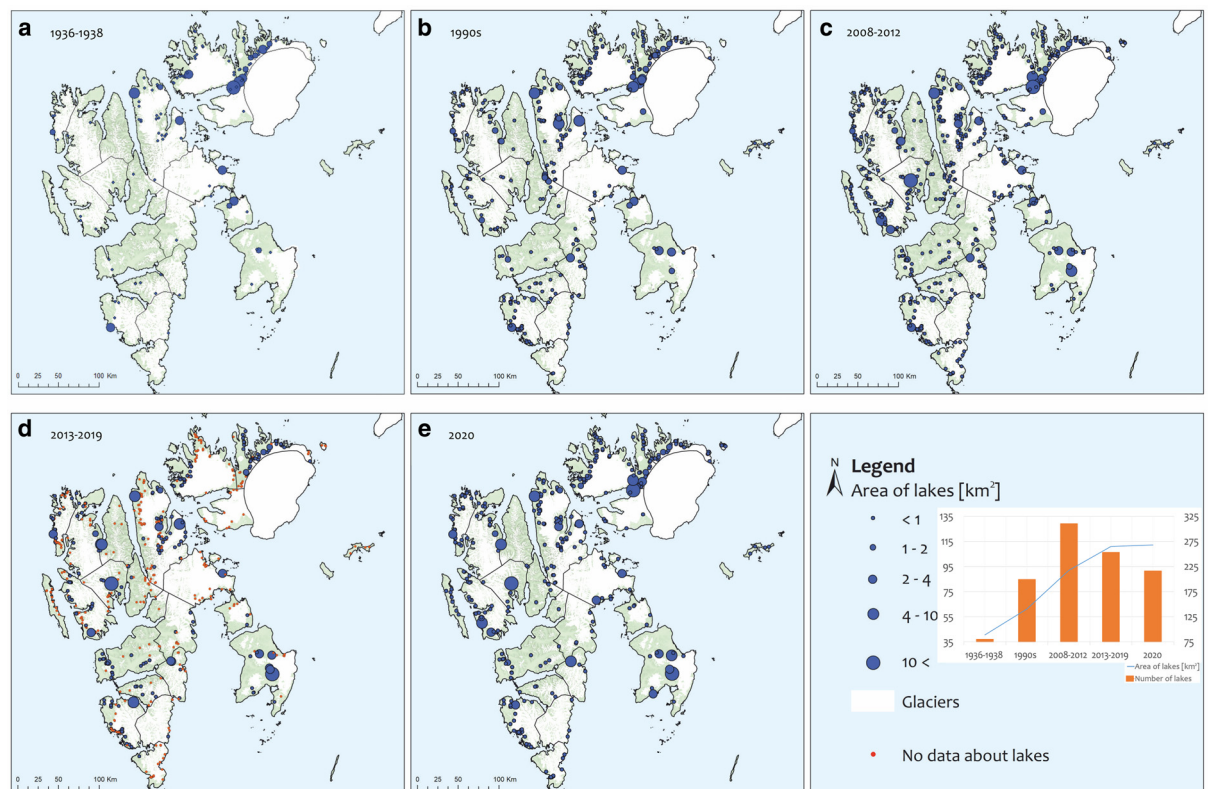
Figure 7. Surface areas of glacial lakes in Svalbard in (a) the 1930s, (b) the 1990s, (c) 2008–2012, (d) 2013–2019, and (e) 2020.
Source: base map from Norwegian Polar Institute.
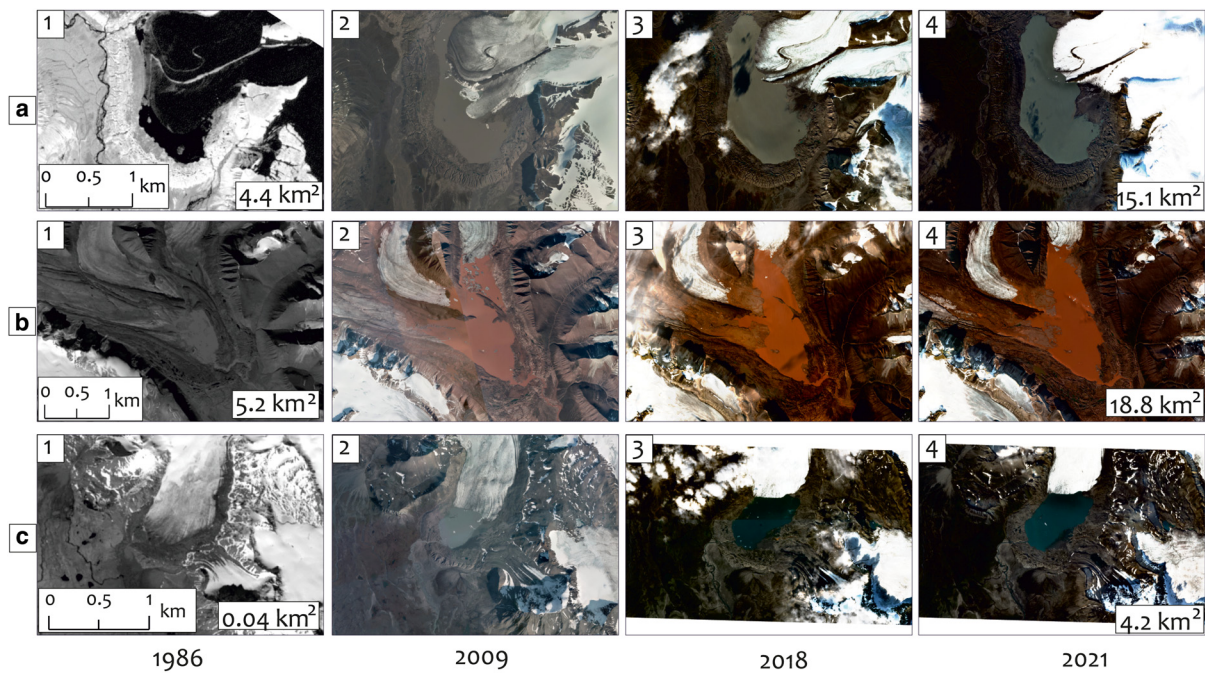
Figure 8. Examples of rapid changes in glacial lakes in Svalbard: (a) Lake Gandvatnet, (b) Lake Trebrevatnet, and (c) Lake Vetterndammen.
Source: based on Sentinel and Landsat satellite images.

Svalbard were relatively stable in terms of annual mass loss or gain (Noël and others, 2020). Since 1985, however, their mass has been in continuous decline, resulting in the cumulative loss of about 350 Gt of ice cover from Svalbard by 2012 (Noël and others, 2020). The rate of glacial mass loss in Svalbard between 2000 and 2019 has been estimated at $-7\ \text{Gt}\ \text{yr}^{-1}$ (Noël and others, 2020). It is therefore lower than the corresponding rate in Alaska ($-75\ \text{Gt}\ \text{yr}^{-1}$), which is the highest worldwide (Jakob and others, 2021; Zemp and others, 2012; Rick and others, 2022), but significantly higher than that in the Himalaya ($-2.86\ \text{Gt}\ \text{yr}^{-1}$) (Kaushik and others, 2022). Thus, if we normalise the rate of deglaciation of the regions listed with respect to the area occupied by glaciers there per 100 km^2, the highest value is invariably found in Alaska ($-0.25\ \text{Gt}\ \text{yr}^{-1}/100\ \text{km}^2$), followed by Svalbard ($-0.02\ \text{Gt}\ \text{yr}^{-1}/100\ \text{km}^2$) and the Himalaya ($-0.01\ \text{Gt}\ \text{yr}^{-1}/100\ \text{km}^2$) (Noël and others, 2020; Jakob and others, 2021; Kaushik and others, 2022; Rick and others, 2022). Glacial ablation allows glacial lakes to form in proglacial zones free of ice (Furian and others, 2021). The ratio of the area of glacial lakes (km^2) to the normalised glaciated area of Svalbard (per 100 km^2) was 0.2 in 1936 but as much as 0.43 in 2010, and despite their rather rapid development (disappearance of glaciers, with a simultaneous increase in lake area), is relatively small compared to Alaska, where the average lake area (km^2) per 100 km^2 of glaciers was between 0.2 and 1.7 (Rick and others, 2022).

Our study highlights two key patterns: (1) There is a clear spatial distribution of different types of glacial lake in Svalbard controlled by geology, and (2) since the 1930s, glacial lakes in Svalbard have experienced phases of fastest growth between 1990s and 2008–2012, which harmonise with temporal patterns in other regions (Shugar and others, 2020; Wang and others, 2020). These patterns are discussed below.

5.1 Spatial distribution of glacial lakes

The proportion of each glacial lake class on Svalbard contrasts with the inventory of glacial lakes in Alaska, which shows that Alaska has a different pattern, where the most frequent glacial lakes are moraine-dammed lakes, followed by bedrock-dammed lakes and lastly ice-dammed lakes (Rick and others, 2022). In high-mountain regions such as the Himalaya, the Andes, the Karakoram and the Alps, where glacial lake inventories have been compiled, such lakes are primarily restricted to *U*-shaped valleys (Zhang and others, 2015; Viani and others, 2016; Buckel and others, 2018; Wilson and others, 2018). This is also in contrast to Svalbard, where glacial lakes are located mainly within moraines which in the archipelago are often located beyond the *U*-shaped valleys.

Based on the data presented, we attribute the spatial variability in glacial lake types in Svalbard to its diverse geology,

Table 4. Types of glacial lakes and their bedrock geology

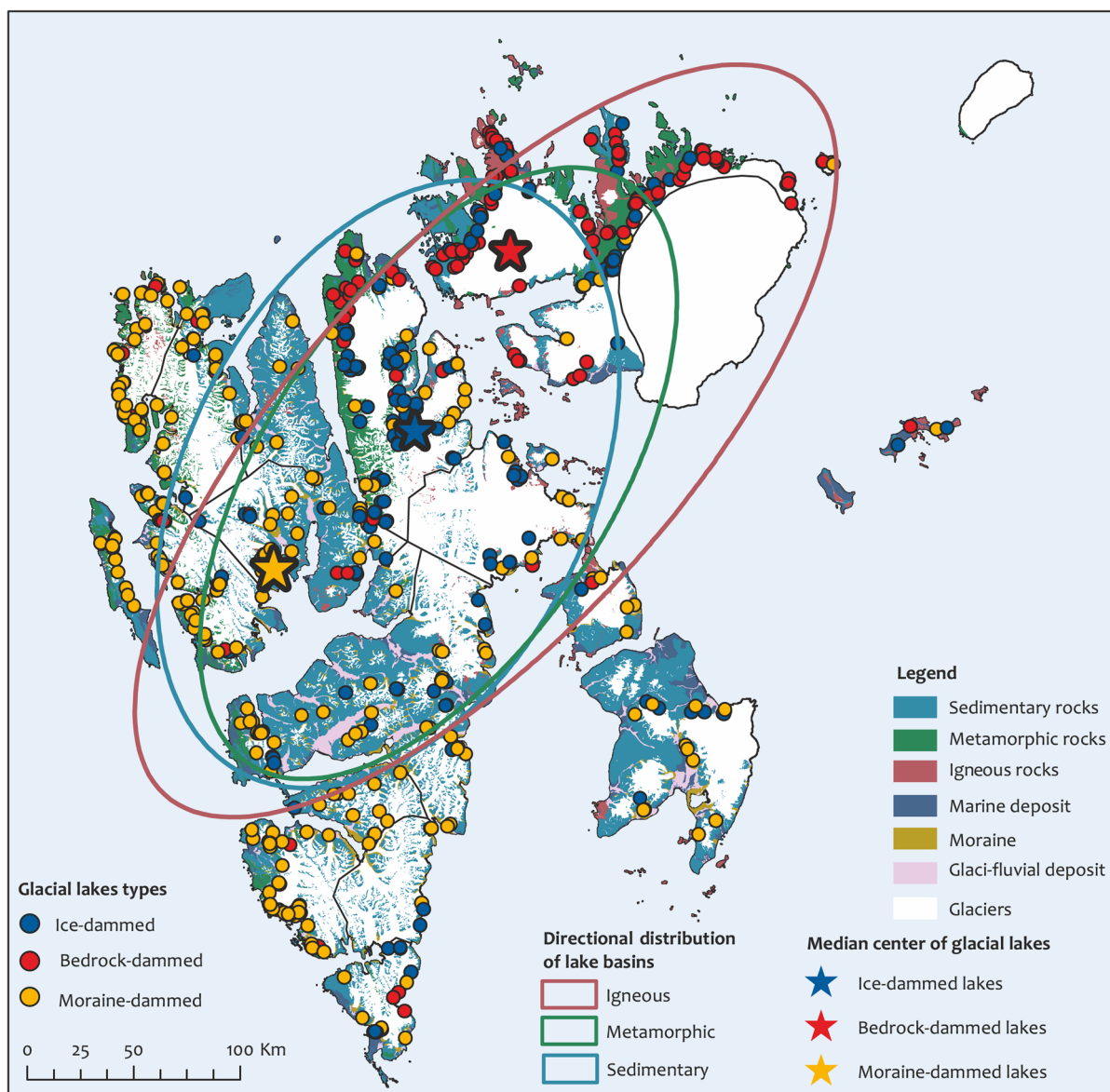|	Glacial lakes types							
	Bedrock-dammed lakes		Ice-dammed lakes		Moraine-dammed lakes		All glacial lake types	
Geology								
Glacio-fluvial deposit	4	4%	3	2%	10	3%	17	3%
Igneous	5	4%	3	2%	13	4%	21	4%
Marine deposit	4	4%	3	2%	6	2%	13	2%
Metamorphic	44	39%	55	34%	61	21%	160	28%
Moraine	34	30%	62	38%	149	51%	245	43%
Sedimentary	22	19%	37	23%	51	18%	110	19%
All types of rocks	**113**	**100%**	**163**	**100%**	**290**	**100%**	**566**	**100%**

Figure 9. Statistical approach of median centres of glacial lake types and their relationship with the directional distribution of lake basins.
Source: base map from Norwegian Polar Institute.

geomorphology and climate. Most of the moraine-dammed lakes lie along the west coast of Spitsbergen, the maritime climate of which is strongly influenced by its proximity to the warm West Spitsbergen Current. This area is dominated by sedimentary rocks (Fig. 8), mountainous topography and experiences frequent paraglacial and periglacial processes, all of which contribute to large amounts of debris falling onto glacier surfaces and, hence, to sediment availability to build end and lateral moraines (de Haas and others, 2015; Eckerstorfer and others, 2017; Rouyet and others, 2021). Water to fill the lakes is abundant along the west coast owing to the highest melt rates of local land-terminating glaciers (Małecki, 2022) and the relatively high level of liquid precipitation (Førland and Hanssen-Bauer, 2000). Glacial lakes on coasts are similarly dominant in Alaska and east Greenland (How and others, 2021; Rick and others, 2022). In contrast, bedrock-dammed and ice-dammed lakes are found mainly to the north-east of Svalbard. In this region, moraines are not so well-developed owing to the limited availability of sediments, which is associated with the glacier type (mainly ice caps) and bedrock lithology (more resistant igneous and metamorphic rocks).

Glacial lakes in Svalbard display similarities to glacial lakes situated in high mountain and polar areas. For instance, the lakes in north-eastern Spitsbergen, where ice-dammed lakes dominate, may well resemble the 'high mountain' glacial lakes in the Andes (Emmer and others, 2020), whereas the moraine-dammed lakes dominating west Spitsbergen have morphological characteristics similar to those of glacial lakes in deep Himalayan valleys (Khadka and others, 2018).

5.2 Temporal changes in glacial lakes

An important finding of this study is the considerable increase of the glacial lake area in Svalbard over the period of study. Among the glacial lakes with complete temporal data coverage (Table 4), this increase was equal to 177% (or 72 km^2) between 1936 and 2020. More recently, the 83% increase (51 km^2) from the 1990s to 2020 sets Svalbard above the global average rate of glacial lake expansion (a 51% increase in area during 1990–2015; Shugar and others, 2020), but not as high as some other high-latitude regions such as Iceland (+142%), Scandinavia (+131%) and Arctic Russia (+152%) (Shugar and others, 2020).
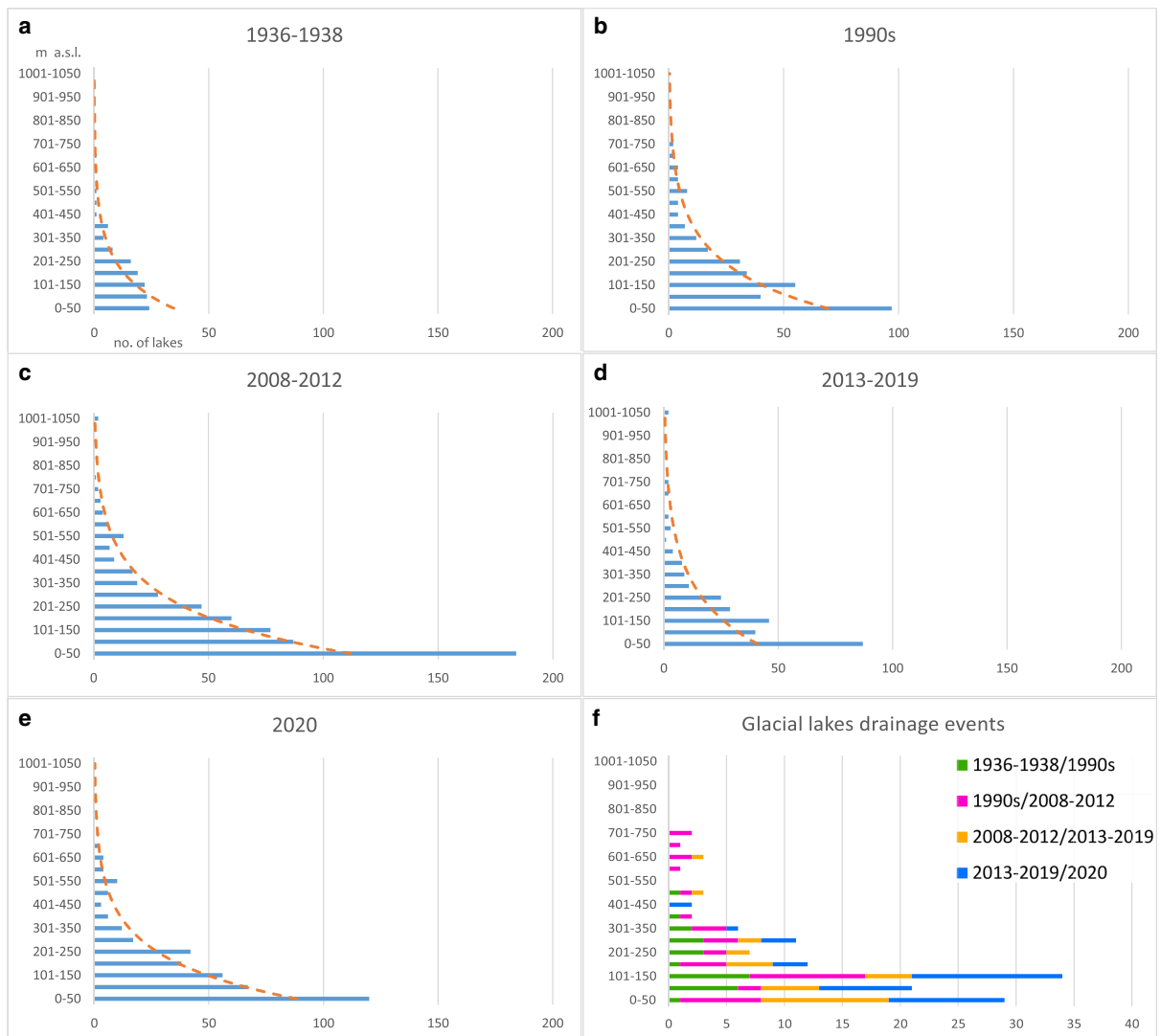
Figure 10. (a–e) Distribution of glacial lakes with 50 m a.s.l. altitude increments. (f) Distribution of the altitude of glacial lakes showing signs of drainage events.

As regards the glacial lakes in Svalbard, the data presented in Table 5 show a post-2012 decline in their overall number. Although the time windows with the best quality data and highest lake count coincide (2008–2012), we argue that the recent decrease in the number of glacial lakes is a true phenomenon. This may be explained by the merging of existing glacial lakes into larger networks and the partial drainage of higher-elevated lakes to supply lower ones. This is in line with the observed increase in the overall area (Table 4), average area (e.g. from $0.13 \, km^2$ in 1936 to $0.30 \, km^2$ in 2020) and median area (e.g. from $0.002 \, km^2$ in 1936 and $0.013 \, km^2$ in 2020). This evolution of Svalbard lakes stands in contrast to the dominant global pattern, as in other regions there appears to be a continuous increase of both lake areas and numbers, such as Greenland between the 1980s and 2017 (How and others, 2021), Alaska between the 1980s and 2010s (Rick and others, 2022) or Nepal between 1987 and 2017 (Khadka and others, 2018). Whether or not a similar reduction in the number of glacial lakes is taking place elsewhere is, however, unclear owing to the different timestamps between existing studies. Nevertheless, this finding highlights the benefit of increased time resolution used in glacial lake research and demonstrates that it enables quantification of shorter term, nonobvious trends in glacial lake evolution.

5.3 Lake drainage events in Svalbard

In the present study, we detected 134 lake drainage events from glacial lakes in Svalbard between the 1930s and 2020. Most events (65) were associated with drainage from moraine-dammed lakes. This is hardly surprising, given that moraine-dammed lakes are the most frequent glacial lake type in Svalbard and exhibit the greatest changes in number and area over the study period. During the summer season, when the water runoff exceeds the retention capacity, water might overtop moraine dams or create moraine breaches, causing lake drainage with a potential for GLOF events (Clague and Evans, 2000; Thompson and others, 2012; Harrison and others, 2018; Veh and others, 2019; Ewertowski and Tomczyk, 2020; Tomczyk and others, 2020; Worni and others, 2014; Cook and others, 2016; Emmer, 2017). Overall, the ratio of detected lake drainage events to the 2008–2012 number of moraine-dammed lakes was 1:4.5. An example of a GLOF event of this class of lake occurred at Lake Trebrevatnet (Fig. 9).

Our observations indicate that ice-dammed lakes might experience even greater seasonal changes than moraine-dammed lakes, which would constitute the greatest GLOF threat in Svalbard. This is mostly due to the susceptibility of ice dams to seasonal changes and their repeated collapse (Prakash and
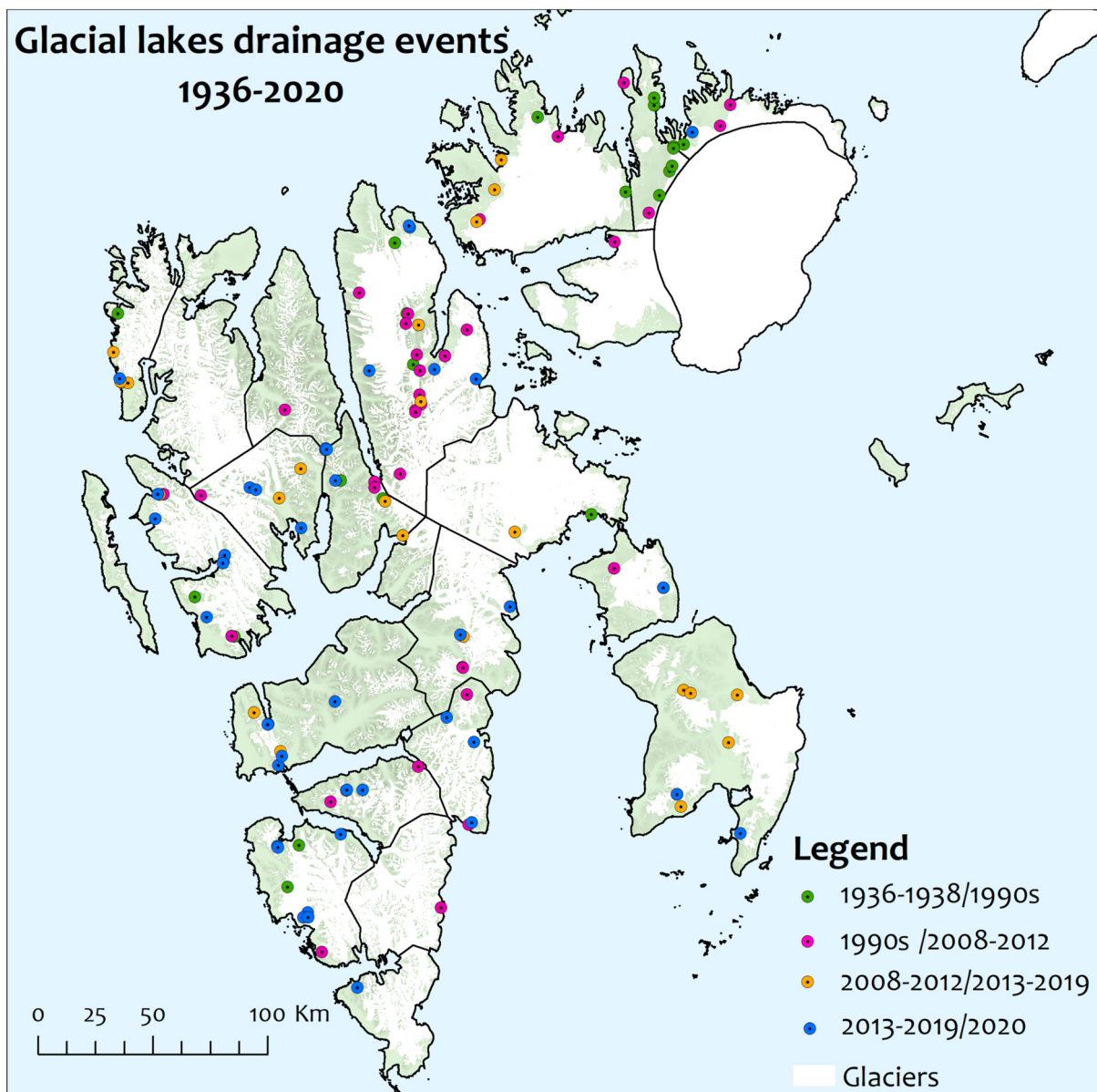
Figure 11. Spatial distribution of glacial lakes drainage events in Svalbard during the period 1936–2020.
Base map from Norwegian Polar Institute (2020b).

Nagarajan, 2018; Bhambri and others, 2020; Lützow and others, 2023; Veh and others, 2023). Among all the ice-dammed lakes in Svalbard, we counted 53 lake drainage events, which resulted in a high lake drainage event-to-lake number ratio of 1:3.0, which corresponds to the anticipated instability of ice-dammed lakes. A good example is Lake Goësvatnet, the best documented ice-dammed lake in Svalbard (NW Sørkapp Land). Until the year 2000, the lake drained through a channel located in the transition zone between dead ice and the active glacier ice of Gåsbreen, followed by its complete disappearance as a result of a GLOF event (Grzes and Banach, 1984; Schoner and Schoner, 1997; Ziaja and Ostafin, 2007; Ziaja and others, 2016). In accounting for the further projected temperature increase over Svalbard (Hanssen-Bauer and others, 2019) and the anticipated acceleration in glacier retreat, we expect similar GLOF events to occur in Svalbard in the coming years and decades, owing to the increasing amounts of water accumulated behind retreating ice dams, particularly in Nordaustlandet and north-eastern Spitsbergen, where ice-dammed lakes are the most numerous (Fig. 8).

Of the other types of glacial lakes on Svalbard, bedrock-dammed lakes are the fewest in number, mostly located in

Table 5. Changes of glacial lakes in Svalbard from the 1930s to 2020

Year	Number of all detected lakes	Area of all detected lakes [km²]	Number of detected lakes with full coverage data (1936–2020)	Area of detected lakes with full coverage data (1936–2020) [km²]
1936–1938	126	74.71 ± 1.78	80	40.50 ± 0.98
1990s	321	109.87 ± 0.17	199	61.16 ± 0.04
2008–2012	566	146.14 ± 0.34	310	91.96 ± 0.1
2013–2019	271	114.90	253	110.92
2020	387	168.83 ± 4.22	216	112.14 ± 1.19

Nordaustlandet and north-eastern Spitsbergen (Fig. 8). The number of detected lake drainage events from bedrock-dammed lakes was the lowest (16), resulting in the lowest lake drainage event-to-lake number ratio of 1:7.0. GLOF events from bedrock-dammed lakes may only occur in response to catastrophic trigger events, such as large calving events, avalanches, mountain slope mass movements or cascading effects due to glacial floods from higher lakes, which are capable of triggering displacement waves overtopping bedrock dams (Carey and others, 2012; Vilímek and others, 2015; Emmer and others, 2016; Vilca and others, 2021). Owing to the generally low ice velocities of most land-terminating glaciers in Svalbard (Małecki, 2022) and the relatively gentle topography in north-eastern Svalbard, we anticipate a low likelihood of GLOFs from bedrock-dammed lakes in the near future.

6. Conclusions

This inventory constitutes a record of 566 glacial lakes in Svalbard (2008–2012) with a total area of 146.14 km^2. The vast majority of the 290 moraine-dammed lakes lie on the west coast of Spitsbergen, whereas the 157 ice-dammed lakes dominate north-eastern Spitsbergen and the 113 bedrock-dammed lakes prevail on Nordaustlandet. The spatial distribution of glacial lakes in Svalbard is interpreted as having resulted from the interplay between local climatic conditions, glacier margin retreat, adjacent landscape features and bedrock lithology. The temporal changes in Svalbard's glacial lakes indicate that they increased in number from the 1930s to 2008–2012, thereafter decreasing to 2020. The total area of glacial lakes increased continuously from the 1930s to 2020. The changes in the area and number of glacial lakes between the 1930s and 2020 also impacted the potential for glacial lake drainage events or GLOFs. A total of 134 glacial lakes that experienced at least partial drainage were identified, and it is anticipated that the frequency of glacial lake drainage events or GLOFs will increase in the future as a result of climate warming and the associated destabilisation of moraines and ice dams. We also argue that our results should initiate a debate on GLOF hazards in Svalbard based on historical occurrence of this events. The observed changes reflect how climate changes affect glacial landscape evolution in Svalbard by accelerating the formation of glacial lakes, leading to higher risks associated with glacial lake drainage events.

Svalbard are available from the NPI (https://toposvalbard.npolar.no/, last access: 15 May 2022 and https://geodata.npolar.no/, last access: 15 May 2022).

References

Aggarwal S, Rai SC, Thakur PK and Emmer A (2017) Inventory and recently increasing GLOF susceptibility of glacial lakes in Sikkim, Eastern Himalaya. *Geomorphology* **295**, 39–54. doi: 10.1016/j.geomorph.2017.06.014

Andreassen LM, Nagy T, Kjøllmoen B and Leigh JR (2022) An inventory of Norway's glaciers and ice-marginal lakes from 2018–19 Sentinel-2 data. *Journal of Glaciology* **68**(272), 1–22. doi: 10.1017/jog.2022.20.

Bhambri R and 9 others (2020) The hazardous 2017–2019 surge and river damming by Shispare Glacier, Karakoram. *Scientific Reports* **10**(4685), 1–14. doi: 10.1038/s41598–020–61277-8.

Buckel J, Otto JC, Prasicek G and Keuschnig M (2018) Glacial lakes in Austria – distribution and formation since the Little Ice Age. *Global and Planetary Change* **164**, 39–51. doi: 10.1016/j.gloplacha.2018.03.003

Carey M, Huggel C, Bury J, Portocarrero C and Haeberli W (2012) An integrated socio-environmental framework for glacier hazard management and climate change adaptation: lessons from lake 513, Cordillera Blanca, Peru. *Climatic Change* **112**, 733–767. doi: 10.1007/s10584-011-0249-8

Carrivick JL and Tweed FS (2013) Proglacial lakes: character, behaviour and geological importance. *Quaternary Science Reviews* **78**, 34–52. doi: 10.1016/j.quascirev.2013.07.028

Carrivick JL, Tweed FS, Sutherland JL and Mallalieu J (2020) Toward numerical modeling of interactions between ice-marginal proglacial lakes and glaciers. *Frontiers in Earth Science* **8**(577068), 1–9. doi: 10.3389/feart.2020.577068

Chen F, Zhang M, Tian B and Li Z (2017) Extraction of glacial lake outlines in Tibet Plateau using Landsat 8 imagery and Google Earth Engine. *IEEE Journal of Selected Topics in Applied Earth Observations and Remote Sensing* **10**(9), 4002–4009. doi: 10.1109/JSTARS.2017.2705718

Clague JJ and Evans SG (2000) A review of catastrophic drainage of moraine-dammed lakes in British Columbia. *Quaternary Science Reviews* **19**, 1763–1783.

Cook SJ, Kougkoulos I, Edwards LA, Dortch J and Hoffmann D (2016) Glacier change and glacial lake outburst flood risk in the Bolivian Andes. *The Cryosphere* **10**(5), 2399–2413. doi: 10.5194/tc-10-2399-2016

Coulombe S and 7 others (2022) Contrasted geomorphological and limnological properties of thermokarst lakes formed in buried glacier ice and ice-wedge polygon terrain. *The Cryosphere* **16**(7), 2837–2857. doi: 10.5194/tc-16-2837-2022

Dallmann WK (2015) Geoscience atlas of Svalbard. *Norwegian Polar Institute Report* **148**, 1–292.

de Haas T, Kleinhans MG, Carbonneau PE, Rubensdotter L and Hauber E (2015) Surface morphology of fans in the high-Arctic periglacial environment of Svalbard: controls and processes. *Earth-Science Reviews* **146**, 163–182. https://doi.org/10.1016/j.earscirev.2015.04.004.

Dudek J, Wieczorek I, Suwiński MK and Strzelecki MC (2022) Multidecadal analysis of paraglacial landscape changes in the foreland of Gåsbreen – Sørkapp Land, Svalbard. *Land Degradation and Development*, 1–31. doi: 10.22541/au.165900615.50507100/v1.

Eckerstorfer E, Malnes E and Christiansen HH (2017) Freeze/thaw conditions at periglacial landforms in Kapp Linné, Svalbard, investigated using field observations, in situ, and radar satellite monitoring. *Geomorphology* **293**, 433–447. http://dx.doi.org/10.1016/j.geomorph.2017.02.010.

Emmer A (2017) Geomorphologically effective floods from moraine-dammed lakes in the Cordillera Blanca, Peru. *Quaternary Science Reviews* **177**, 220–234. doi: 10.1016/j.quascirev.2017.10.028

Emmer A and 5 others (2020) 70 years of lake evolution and glacial lake outburst floods in the Cordillera Blanca (Peru) and implications for the future. *Geomorphology* **365**, 107178. doi: 10.1016/j.geomorph.2020.107178

Emmer A and 36 others (2022) Progress and challenges in glacial lake outburst flood research (2017–2021): a research community perspective. *Natural Hazards and Earth System Sciences* **22**, 3041–3061. doi: 10.5194/nhess-22-3041-2022

Emmer A, Klimeš J, Mergili M, Vilímek V and Cochachin A (2016) 882 lakes of the Cordillera Blanca: an inventory, classification, evolution and assessment of susceptibility to outburst floods. *Catena* **147**, 269–279. doi: 10.1016/j.catena.2016.07.032

Evans IS (2011) Glacier distribution and direction in Svalbard, Axel Heiberg Island and throughout the Arctic: general northward tendencies. *Polish Polar Research* **32**(3), 199–238. doi: 10.2478/v10183-011-0015-7

Ewertowski MW and Tomczyk AM (2020) Reactivation of temporarily stabilized ice-cored moraines in front of polythermal glaciers: Gravitational mass movements as the most important geomorphological agents for the redistribution of sediments (a case study from Ebbabreen and Ragnarbreen, Svalbard). *Geomorphology* **350**, 106952. doi: 10.1016/j.geomorph.2019.106952

Farnsworth WR, Ingólfsson Ó, Retelle M and Schomacker A (2016) Over 400 previously undocumented Svalbard surge-type glaciers identified. *Geomorphology* **264**, 52–60. doi: 10.1016/j.geomorph.2016.03.025

Fitzsimons S and Howarth J (2018) Glaciolacustrine processes. In Menzies J & van der Meer JJM (eds) *Past Glacial Environments*. Amsterdam: Elsevier, pp. 309–334. doi: 10.1016/B978-0-08-100524-8.00009-9.

Førland EJ, Benestad R, Hanssen-Bauer I, Haugen JE and Skaugen TE (2011) Temperature and Precipitation Development at Svalbard 1900–2100. *Advances in Meteorology* **2011**, 1–14. doi: 10.1155/2011/893790

Førland EJ and Hanssen-Bauer I (2000) Increased precipitation in the Norwegian Arctic: True or false? *Climatic Change* **46**(4), 485–509. doi: 10.1023/A:1005613304674

Furian W, Loibl D and Schneider C (2021) Future glacial lakes in High Mountain Asia: an inventory and assessment of hazard potential from surrounding slopes. *Journal of Glaciology* **67**(264), 653–670. doi: 10.1017/jog.2021.18

Geyman EC, van Pelt WJJ, Maloof AC, Aas HF and Kohler J (2022) Historical glacier change on Svalbard predicts doubling of mass loss by 2100. *Nature* **601**(7893), 374–379. doi: 10.1038/s41586-021-04314-4

Govindha Raj BK and Kumar VK (2016) Inventory of glacial lakes and its evolution in Uttarakhand Himalaya using time series satellite data. *Journal of the Indian Society of Remote Sensing* **44**(6), 959–976. doi: 10.1007/s12524-016-0560-y

Govindha Raj BK, Kumar VK and Remya SN (2013) Remote sensing-based inventory of glacial lakes in Sikkim Himalaya: semi-automated approach using satellite data. *Geomatics, Natural Hazards and Risk* **4**(3), 241–253. doi: 10.1080/19475705.2012.707153

Grześ M and Banach M (1984) The origin and evolution of the Goes Lake in Sorkapp Land, Spitsbergen. *Polish Polar Research* **5**(3–4), 241–253.

Hagen JO, Liestøl O, Roland E and Jørgensen T (1993) Glacier atlas of Svalbard and Jan Mayen. *Norwegian Polar Institute meddelelser* 129, 169 pp.

Hanssen-Bauer I and 5 others (2019) Climate in Svalbard 2100 - a knowledge base for climate adaptation. *Norwegian Centre for Climate Services report* 1/2019, 105 pp.

Harrison S and 14 others (2018) Climate change and the global pattern of moraine-dammed glacial lake outburst floods. *The Cryosphere* **12**(4), 1195–1209. doi: 10.5194/tc-12-1195-2018

Holm TM and 6 others (2012) Rapid physicochemical changes in the high Arctic Lake Kongressvatn caused by recent climate change. *Aquatic Sciences* **74**(3), 385–395. doi: 10.1007/s00027-011-0229-0

How P and 10 others (2021) Greenland-wide inventory of ice marginal lakes using a multi-method approach. *Scientific Reports* **11**(1), 1–13. doi: 10.1038/s41598-021-83509-1

Humlum O, Instanes A and Sollid JL (2003) Permafrost in Svalbard: a review of research history, climatic background and engineering challenges. *Polar Research* **22**(2), 191–215. doi: 10.1111/j.1751-8369.2003.tb00107.x

Huss M, Bauder A, Werder M, Funk M and Hock R (2009) Glacier-dammed lake outburst events of Gornersee, Switzerland. *Mitteilungen der Versuchsanstalt für Wasserbau, Hydrologie und Glaziologie an der Eidgenossischen Technischen Hochschule Zürich* **53**(213), 65–84.

Isaksen K and 5 others (2016) Recent warming on Spitsbergen – influence of atmospheric circulation and sea ice cover. *Journal of Geophysical Research: Atmospheres* **121**, 3446–3464. doi: 10.1002/2016JD025606.

Isaksen K and 15 others (2022) Exceptional warming over the Barents area. *Scientific Reports* **12**, 9371. doi: 10.1038/s41598-022-13568-5

Jain SK, Lohani AK, Singh RD, Chaudhary A and Thakural LN (2012) Glacial lakes and glacial lake outburst flood in a Himalayan basin using remote sensing and GIS. *Natural Hazards* **62**(3), 887–899. doi: 10.1007/s11069-012-0120-x

Jakob L, Gourmelen N, Ewart M and Plummer S (2021) Spatially and temporally resolved ice loss in High Mountain Asia and the Gulf of Alaska observed by CryoSat-2 swath altimetry between 2010 and 2019. *The Cryosphere* **15**, 1845–1862. doi: 10.5194/tc-15-1845-2021

Kaushik S, Singh T and Joshi PK (2022) Long-term spatiotemporal variability in the surface velocity of Eastern Himalayan glaciers, India. *Earth Surface Processes and Landforms* **47**(7), 1720–1733. doi: 10.1002/esp.5342

Kavan J and 5 others (2022) Estimating suspended sediment fluxes from the largest glacial lake in Svalbard to fjord system using Sentinel-2 data: Trebrevatnet case study. *Water* **14**(2), 1840. doi: 10.3390/w14121840

Khadka N, Zhang G and Thakuri S (2018) Glacial lakes in the Nepal Himalaya: inventory and decadal dynamics (1977–2017). *Remote Sensing* **10**(12), 1913. doi: 10.3390/rs10121913

Loriaux T and Casassa G (2013) Evolution of glacial lakes from the Northern Patagonia Icefield and terrestrial water storage in a sea-level rise context. *Global and Planetary Change* **102**, 33–40. doi: 10.1016/j.gloplacha.2012.12.012

Luo W, Zhang G, Chen W and Xu F (2020) Response of glacial lakes to glacier and climate changes in the western Nyainqentanglha range. *Science of the Total Environment* **735**, 139607. doi: 10.1016/j.scitotenv.2020.139607

Lützow N, Veh G and Korup O (2023) A global database of historic glacier lake outburst floods[preprint] *Earth System Science Data*, 1–27. doi: 10.5194/essd-2022-449.

Mal S, Kumar A, Bhambri R, Schickhoff U and Singh RB (2020) Inventory and spatial distribution of glacial lakes in Arunachal Pradesh, Eastern Himalaya, India. *Journal of the Geological Society of India* **96**(6), 609–615. doi: 10.1007/s12594-020-1610-1

Małecki J (2016) Accelerating retreat and high-elevation thinning of glaciers in central Spitsbergen. *The Cryosphere* **10**(3), 1317–1329. doi: 10.5194/tc-10-1317-2016

Małecki J (2022) Recent contrasting behaviour of mountain glaciers across the European High Arctic revealed by ArcticDEM data. *The Cryosphere* **16**, 2067–2082. doi: 10.5194/tc-16-2067-2022

Mallalieu J, Carrivick JL, Quincey DJ and Raby CL (2021) Ice-marginal lakes associated with enhanced recession of the Greenland ice sheet. *Global and Planetary Change* **202**, 103503. doi: 10.1016/j.gloplacha.2021.103503

Moreno-Ibáñez M, Hagen JO, Hübner C, Lihavainen H and Zaborska A (2020) *Sess Report* 2020. Svalbard Integrated Arctic Earth Observing Service. 40 pp.

Nie Y and 6 others (2017) A regional-scale assessment of Himalayan glacial lake changes using satellite observations from 1990 to 2015. *Remote Sensing of Environment* **189**, 1–13. doi: 10.1016/j.rse.2016.11.008

Noël B and 10 others (2020) Low elevation of Svalbard glaciers drives high mass loss variability. *Nature Communications* **11**, 4597. doi: 10.1038/s41467-020-18356-1

Nordli Ø, Przybylak R, Ogilvie AEJ and Isaksen K (2014) Long-term temperature trends and variability on Spitsbergen: the extended Svalbard Airport temperature series, 1898–2012. *Polar Research* **33**, 21349. doi: 10.3402/polar.v33.21349

Norwegian Polar Institute (2020a) TopoSvalbard. Available at https://toposvalbard.npolar.no/ (last access: 15 May 2022).

Norwegian Polar Institute (2020b) Norwegian Polar Institute Map Data and Services. Available at https://geodata.npolar.no/ (last access: 15 May 2022).

Nuth C and 7 others (2013) Decadal changes from a multi-temporal glacier inventory of Svalbard. *The Cryosphere* **7**(5), 1603–1621. doi: 10.5194/tc-7-1603-2013

Pfeffer WT and 18 others (2014) The Randolph Glacier Inventory: a globally complete inventory of glaciers. *Journal of Glaciology* **60**(221), 537–552. doi: 10.3189/2014JoG13J176

Post A and Mayo LR (1970) Glacier dammed lakes and outburst floods in Alaska. *Hydrologic Investigations Atlas* **455**, 1–10.

Prakash C and Nagarajan R (2017) Outburst susceptibility assessment of moraine-dammed lakes in Western Himalaya using an analytic hierarchy process. *Earth Surface Processes and Landforms* **42**(14), 2306–2321. doi: 10.1002/esp.4185

Prakash C and Nagarajan R (2018) Glacial lake changes and outburst flood hazard in Chandra basin, North-Western Indian Himalaya. *Geomatics, Natural Hazards and Risk* **9**(1), 337–355. doi: 10.1080/19475705.2018.1445663

Rachlewicz G, Szczuciński W and Ewertowski M (2007) Post-"Little ice age" retreat rates of glaciers around Billefjorden in central Spitsbergen, Svalbard. *Polish Polar Research* **28**(3), 159–186.

Rajaram R, Ganeshkumar A and Partheeban EC (2023) Ecological risk assessment of metals in the Arctic environment with emphasis on Kongsfjorden Fjord and freshwater lakes of Ny-Ålesund, Svalbard. *Chemosphere* **310**, 136737. doi: 10.1016/j.chemosphere.2022.136737.

Rantanen M and 7 others (2022) The Arctic has warmed nearly four times faster than the globe since 1979. *Communications Earth and Environment* **3**, 168. doi: 10.1038/s43247-022-00498-3

Rick B, Mcgrath D, Armstrong W and Mccoy SW (2022) Dam type and lake location characterize ice-marginal lake area change in Alaska and NW Canada between 1984 and 2019. *Cryosphere* **16**(1), 297–314. doi: 10.5194/tc-16-297-2022

Røthe TO, Bakke J, Støren EWN and Bradley RS (2018) Reconstructing Holocene glacier and climate fluctuations from lake sediments in Vårfluesjøen, Northern Spitsbergen. *Frontiers in Earth Science* **6**, 91. doi: 10.3389/feart.2018.00091

Rouyet L and 5 others (2021) Seasonal InSAR displacements documenting the active layer freeze and thaw progression in Central-Western Spitsbergen, Svalbard. *Remote Sensing* **13**(15), 2977. doi: 10.3390/rs13152977

Ruman M and 5 others (2021) A high-Arctic flow-through lake system hydrochemical changes: Revvatnet, southwestern Svalbard (years 2010–2018). *Chemosphere* **275**, 130046. doi: 10.1016/j.chemosphere.2021.130046

Schoner W and Schoner M (1997) Effects of glacier retreat on the outbursts of Goesvatnet, southwest Spitsbergen, Svalbard. *Journal of Glaciology* **43**(144), 276–282. doi: 10.1017/S0022143000003221

Schuler TV and 12 others (2020) Reconciling Svalbard Glacier Mass Balance. *Frontiers in Earth Science* **8**, 156. doi: 10.3389/feart.2020.00156

Senese A and 13 others (2018) Inventory of glaciers and glacial lakes of the central Karakoram national park (CKNP – Pakistan). *Journal of Maps* **14**(2), 189–198. doi: 10.1080/17445647.2018.1445561

Sentinel Hub. Available at https://www.sentinel-hub.com. Sinergise Ltd (last access: 15 May 2022).

Sessford EG, Strzelecki MC and Hormes A (2015) Reconstruction of Holocene patterns of change in a High Arctic coastal landscape, Southern Sassenfjorden, Svalbard. *Geomorphology* **234**, 98–107. doi: 10.1016/j.geomorph.2014.12.046

Sevestre H, Benn DI, Hulton NRJ and Bælum K (2015) Thermal structure of Svalbard glaciers and implications for thermal switch models of glacier surging. *Journal of Geophysical Research: Earth Surface* **120**(10), 2220–2236. doi: 10.1002/2015JF003517

Shugar DH and 9 others (2020) Rapid worldwide growth of glacial lakes since 1990. *Nature Climate Change* **10**(10), 939–945. doi: 10.1038/s41558-020-0855-4

Sobota I (2014) Changes in dynamics and runoff from the High Arctic glacial catchment of Waldemarbreen, Svalbard. *Geomorphology* **212**, 16–27. doi: 10.1016/j.geomorph.2013.04.001

Sobota I, Nowak M and Weckwerth P (2016) Long-term changes of glaciers in north-western Spitsbergen. *Global and Planetary Change* **144**, 182–197. doi: 10.1016/j.gloplacha.2016.07.006

Strzelecki MC, Long AJ and Lloyd JM (2017) Post-Little Ice Age development of a high arctic paraglacial beach complex. *Permafrost and Periglacial Processes* **28**, 4–17. doi: 10.1002/ppp.1879

Thompson SS, Benn DI, Dennis K and Luckman A (2012) A rapidly growing moraine-dammed glacial lake on Ngozumpa Glacier, Nepal. *Geomorphology* **145–146**, 1–11. doi: 10.1016/j.geomorph.2011.08.015

Tomczyk AM, Ewertowski MW and Carrivick JL (2020) Geomorphological impacts of a glacier lake outburst flood in the high arctic Zackenberg river, NE Greenland. *Journal of Hydrology* **591**, 125300. doi: 10.1016/j.jhydrol.2020.125300

Ukita J and 10 others (2011) Glacial lake inventory of Bhutan using ALOS data: methods and preliminary results. *Annals of Glaciology* **52**(58), 65–71. doi: 10.3189/172756411797252293

van der Bilt WGM, D'Andrea WJ, Werner JP and Bakke J (2019) Early Holocene temperature oscillations exceed amplitude of observed and projected warming in Svalbard lakes. *Geophysical Research Letters* **46**(24), 14732–14741. doi: 10.1029/2019GL084384

Veh G and 8 others (2023) Less extreme and earlier outbursts of ice-dammed lakes since 1900. *Nature* **614**, 701–720. doi: 10.1038/s41586-022-05642-9

Veh G, Korup O, von Specht S, Roessner S and Walz A (2019) Unchanged frequency of moraine-dammed glacial lake outburst floods in the Himalaya. *Nature Climate Change* **9**(5), 379–383. doi: 10.1038/s41558-019-0437-5

Viani C, Giardino M, Huggel C, Perotti L and Mortara G (2016) An overview of glacier lakes in the Western Italian Alps from 1927 to 2014 based on multiple data sources (historical maps, orthophotos and reports of the glaciological surveys). *Geografia Fisica e Dinamica Quaternaria* **39**(2), 203–214. doi: 10.4461/GFDQ2016.39.19

Vilca O, Mergili M, Emmer A, Holger F and Huggel C (2021) The 2020 glacial lake outburst flood process chain at Lake Salkantaycocha (Cordillera Vilcabamba, Peru). *Landslides* **18**, 2211–2223. doi: 10.1007/s10346-021-01670-0

Vilímek V, Klimeš J, Emmer A and Benešová M (2015) Geomorphologic impacts of the glacial lake outburst flood from Lake No. 513 (Peru). *Environmental Earth Sciences* **73**(9), 5233–5244. doi: 10.1007/s12665-014-3768-6

Wang X and 9 others (2020) Glacial lake inventory of High Mountain Asia (1990–2018) derived from Landsat images. *Earth System Science Data* **12**, 2169–2182. doi: 10.5194/essd-12-2169-2020

Wawrzyniak T and Osuch M (2020) A 40-year High Arctic climatological dataset of the Polish Polar Station Hornsund (SW Spitsbergen, Svalbard). *Earth System Science Data* **12**(2), 805–815. doi: 10.5194/essd-12-805-2020

Wilson R and 6 others (2018) Glacial lakes of the Central and Patagonian Andes. *Global and Planetary Change* **162**, 275–291. doi: 10.1016/j.gloplacha.2018.01.004

Worni R, Huggel C, Clague JJ, Schaub Y and Stoffel M (2014) Coupling glacial lake impact, dam breach, and flood processes: a modeling perspective. *Geomorphology* **224**, 161–176. doi: 10.1016/j.geomorph.2014.06.031

Worni R, Huggel C and Stoffel M (2013) Glacial lakes in the Indian Himalayas – from an area-wide glacial lake inventory to on-site and modeling based risk assessment of critical glacial lakes. *Science of the Total Environment* **468-469**, 71–84. doi: 10.1016/j.scitotenv.2012.11.043

Yao X, Liu S, Han L and Sun M (2018) Definition and classification systems of glacial lake for inventory and hazards study. *Journal of Geographical Sciences* **28**(2), 193–205. doi: 10.1007/s11442-018-1467-z

Zemp M and 6 others (2012) Fluctuations of Glaciers 2005–2010. *World Glacier Monitoring Service, Zurich, Switzerland* X, 336. doi: 10.5904/wgms-fog-2014-09

Zhang G, Yao T, Xie H, Wang W and Yang W (2015) An inventory of glacial lakes in the Third Pole region and their changes in response to global warming. *Global and Planetary Change* **131**, 148–157. doi: 10.1016/j.gloplacha.2015.05.013

Ziaja W, Dudek J and Ostafin K (2016) Landscape transformation under the Gåsbreen glacier recession since 1899, southwestern Spitsbergen. *Polish Polar Research* **37**(2), 155–172. doi: 10.1515/popore-2016-0010

Ziaja W and Ostafin K (2007) Współczesna przemiana przemiana krajobrazu lodowca Gas i okolicy. *Abiotyczne środowisko Spitsbergenu w latach* 2005–2006 *w warunkach globalnego ocieplenia*, 235–245.